

Tamara Fletcher  
Institute of Applied Ecology  
Chinese Academy of Sciences  
72 Wenhua Rd,  
Shenyang, Liaoning, 110164

15 May 2019

Dear Prof. Reyes,

Please find below our point-by-point reply to the suggested revisions to our manuscript, cp-2018-60, "Evidence for fire in the Pliocene Arctic in response to amplified temperature" for publication in *Climate of the Past*.

The substantive changes are early in the section 4.2, where we have developed the section on fire as a feedback to climate and simplified the section on climate as a feedback to fire, following your suggestions.

Thank you for the time you have invested in this manuscript, and I hope the changes make this manuscript suitable for publication in *Climate of the Past*.

Sincerely,



Tamara Fletcher (On behalf of the authorship team)

**Editor Decision: Publish subject to minor revisions (review by editor) (29 Apr 2019)**

by Alberto Reyes

Comments to the Author:

Dear Dr. Fletcher,

Thank you for the submission of a revised version of your manuscript on fire in the Pliocene forests of Ellesmere Island. Your decision to remove the CO<sub>2</sub> reconstruction from the manuscript removes many of the contentious points that were raised in review, and at this point I'm keen to move forward with publishing your manuscript subject to some minor revision. I'm still concerned that Dana Royer's earlier concerns about the feedback angle in the manuscript haven't been fully dealt with, but I think this can be addressed with minor revision. I also have some other suggestions for minor revision, mostly for clarity, which are detailed below.

line 31: "much greater than present...."

RE: [This sentence has been edited.](#)

Lines 65-67: Please check for more recent relevant literature on efforts to model warm intervals such as the Pliocene – a good starting point is the PlioMIP2 website. Depending on your assessment of newer literature, you might want to revise the next two sentences too.

RE: [This section has been updated with results from PlioMIP2 published since submitting this manuscript.](#)

Line 157: "charcoal counts" seems more appropriate?

RE: [This has been changed to specify counts and measurements.](#)

Line 204: "it has been"... "it" could refer to several things in this context – please clarify.

RE: [This sentence has been edited for clarity.](#)

Section 2.3: Please provide a brief explanation of how uncertainty is treated (both with reconstruction uncertainty and propagated analytical uncertainty). Ref. 1 picked up on this point too.

RE: [The RMSE are reported in the equations \(3, 4 and 5\), and the derivation of these is found in the citations given \(Pearson et al. 2011; Russel et al. 2018\). The analytical uncertainty is now reported at the end of 2.3](#)

Line 433: " 1 cm<sup>3</sup>"

RE: [This change has been made.](#)

Line 444: "...grid cells, was counted..."

RE: [This has been changed. "...was tabulated".](#)

Lines 650 and 651: I assume the quoted MAAT and MST are mean +/- stdev for n stratigraphic intervals? Please clarify, and provide the n.

RE: The n=34 is now reported at 296 of the mark-up version, and average is changed to mean for specificity. This n-value matches description of the sample layers used for each analysis given in section 2.1 *"temperature estimates from specific bacterial membrane lipids were taken from 22 of the sample layers collected in 2006 and an additional 12 samples collected in 2010"*.

Line 678: "definitively" not "definitely"

RE: This change has been made.

Line 711: "have" not "has"

RE: This change has been made.

Line 728: seems like a good spot to refer to Fig S3

RE: This has been added.

Line 899: "...suggests mean reconstructed summer temperatures were..."

RE: This change has been made.

Lines 900-907: This section is pretty awkward. The caveat about comparing Pliocene-modern differences in MST vs MAT is a point well taken, the execution is clunky and needs careful wordsmithing. Similarly, the last sentence is a good point but needs some massaging.

RE: I have substantially edited and simplified this section.

Line 948: unclear what is meant by "causatively here"

RE: This has been reworded for clarity.

Line 962: "...low concentration of charcoal in this stratigraphic interval..."

RE: This change has been made.

Line 967-970: use commas to separate clauses in this sentence

RE: This change has been made.

Line 997: do you mean Castor? Or the extinct taxon Dipoides?

RE: This change has been made.

Lines 1010-1012: minor editing to clarify what the many "it" occurrences refer to.

RE: This change has been made.

Lines 1027-1029: This is really just a snapshot in time, so I suggest being a little more equivocal: "Thus, while vegetation and fire regimes seemingly changed through time....." and "...have no apparent trend, within analytical and reconstruction uncertainty."

RE: This change has been made.

Line 1033: "...change in vegetation community"

RE: This change has been made.

Line 1034: what is a fine fuel load? Do you mean fire fuel load?

RE: This is now specified.

Line 1044-1050: This bit on fire and feedback comes as a bit of a surprise at this point in the manuscript. It's also pretty underdeveloped. Is there not more literature to support the contention of a potential feedback to climate warming in a forested High Arctic?

RE: This section now follows paragraph two of the discussion section 4.2. It has been revised to include examples from the literature on modern modelling and observational work related to fire's impact on climate in the high northern latitudes. Most Pliocene climate models have not explicitly evaluated fire, and so coverage of this is necessarily brief.

Line 1053: Careful with the snapshot nature of this study when referring to "the Pliocene"

RE: Specifics have now been added.

Line 1057: suggest omitting "as a feedback" here

RE: This has now been deleted.

1 Evidence for fire in the Pliocene Arctic in response to amplified temperature

2 Tamara Fletcher<sup>1\*</sup>, Lisa Warden<sup>2\*</sup>, Jaap S. Sinninghe Damsté<sup>2,3</sup>, Kendrick J. Brown<sup>4,5</sup>, Natalia  
3 Rybczynski<sup>6,7</sup>, John Gosse<sup>8</sup>, and Ashley P Ballantyne<sup>1</sup>

4 <sup>1</sup> College of Forestry and Conservation, University of Montana, Missoula, 59812, USA

5 <sup>2</sup> Department of Marine Microbiology and Biogeochemistry, NIOZ Royal Netherlands Institute for Sea Research, Den  
6 Berg, 1790, Netherlands

7 <sup>3</sup> Department of Earth Sciences, University of Utrecht, Utrecht, 3508, Netherlands

8 <sup>4</sup> Natural Resources Canada, Canadian Forest Service, Victoria, V8Z 1M5, Canada

9 <sup>5</sup> Department of Earth, Environmental and Geographic Science, University of British Columbia Okanagan, Kelowna,  
10 V1V 1V7, Canada

11 <sup>6</sup> Department of Palaeobiology, Canadian Museum of Nature, Ottawa, K1P 6P4, Canada

12 <sup>7</sup> Department of Biology & Department of Earth Sciences, Carleton University, Ottawa, K1S 5B6, Canada

13 <sup>8</sup> Department of Earth Sciences, Dalhousie University, Halifax, B3H 4R2, Canada

14 \*Authors contributed equally to this work

15 Correspondence to: Tamara Fletcher ([tamara.fletcher@umontana.edu](mailto:tamara.fletcher@umontana.edu))

16 **Abstract.** The mid-Pliocene is a valuable time interval for investigating equilibrium climate at current atmospheric  
17 CO<sub>2</sub> concentrations, because atmospheric CO<sub>2</sub> concentrations are thought to have been comparable to current day and  
18 yet the climate and distribution of ecosystems were quite different. One intriguing, but not fully understood, feature

19 of the early to mid-Pliocene climate is the amplified arctic temperature response and its impact on arctic ecosystems.  
20 Only the most recent models appear to correctly estimate the degree of warming in the Pliocene Arctic and validation  
21 of the currently proposed feedbacks is limited by scarce terrestrial records of climate and environment. Here we  
22 reconstruct the summer temperature and fire regime from a sub-fossil fen-peat deposit on west-central Ellesmere  
23 Island, Canada, that has been chronologically constrained using cosmogenic nuclide burial dating to 3.9 ± 1.5/-0.5 Ma.

24 The estimate for average mean summer temperature is 15.4 ± 0.8°C using specific bacterial membrane lipids, i.e.  
25 branched glycerol dialkyl glycerol tetraethers. This is above the proposed threshold that predicts a substantial increase  
26 in wildfire in the modern high-latitudes. Macro-charcoal was present in all samples from this Pliocene section with  
27 notably higher charcoal concentration in the upper part of the sequence. This change in charcoal was synchronous  
28 with a change in vegetation that included an increase in abundance of fire-promoting *Pinus* and *Picea*. Paleovegetation  
29 reconstructions are consistent with warm summer temperatures, relatively low summer precipitation and an incidence  
30 of fire comparable to fire adapted boreal forests of North America, and central Siberia.

31 To our knowledge, this site provides the northern-most evidence of fire during the Pliocene. It suggests that ecosystem  
32 productivity was greater than present-day, providing fuel for wildfires, and that the climate was conducive to the  
33 ignition of fire during this period. The results reveal interactions between paleovegetation and paleoclimate were  
34 mediated by fire in the High Arctic during the Pliocene, even though CO<sub>2</sub> concentrations were similar to modern.

Deleted: as

Deleted: Current

Deleted: underestimate

Deleted: radionuclide

Deleted: that saw

Deleted: increase in abundance

Deleted: or potentially

Deleted:

Deleted: much

Deleted: This study indicates

Deleted: that

## 46 1 Introduction

47 Current rates of warming in the Canadian Arctic are now roughly triple the rate of global warming (Bush and Lemmen,  
48 2019). Since 1850, global land surface temperatures have increased by approximately 1.0°C, whereas circum-arctic  
49 land surface temperatures have increased by >2.0°C (Jones and Moberg, 2003; Francis and Skific, 2015). Such arctic  
50 amplification of temperatures has also occurred during other warm climate anomalies in Earth's past. Paleoclimate  
51 records from the Arctic indicate that the change in arctic summer temperatures during past global warm periods was  
52 3–4 times larger than global temperature change (Miller et al., 2010). While earth system models (ESMs) have been  
53 able to provide fairly accurate predictions of the modern amplification of arctic temperatures hitherto observed for  
54 some time (Marshall et al., 2014), they have only recently implemented mechanisms that simulate Arctic amplification  
55 of temperature for past warm periods such as the Pliocene (2.6–5.3) with a convincing pattern of seasonality (Zheng  
56 et al. 2019). The success of earlier models at capturing modern warming, contrasted with the additions needed to  
57 simulate the Pliocene Arctic temperatures, suggest that the array of fast and slow feedback mechanisms have not fully  
58 manifested for the modern Arctic, and perhaps there are still further feedback mechanisms we are yet to understand  
59 and implement in climate models.

60 The Pliocene is an intriguing climatic interval that offers important insights into climate feedbacks. Atmospheric  
61 CO<sub>2</sub> concentrations were, at times, as high as modern (Fig. 1), but generally show a decreasing trend throughout the  
62 Pliocene (Haywood et al., 2016; Pagani et al., 2010; Royer et al., 2007; Stap et al., 2016). Although CO<sub>2</sub> estimates  
63 from different methods do not converge, the modelled direct effects of these CO<sub>2</sub> discrepancies appear to be small  
64 (Feng et al., 2017). Of additional importance for comparability to the modern climate system, continental  
65 configurations were similar to present (Dowsett et al., 2016). While global mean annual temperatures (MATs) during  
66 the Pliocene were only ~ 3°C warmer than present day, arctic land surface MATs may have been as much as 15 to  
67 22°C warmer (Ballantyne et al., 2010; Csank et al., 2011a; Csank et al., 2011b; Fletcher et al., 2017). Further, arctic  
68 sea surface temperatures may have been as much as 10 to 15°C warmer than modern (Robinson, 2009), and sea-levels  
69 were approximately 25m higher than present (Dowsett et al., 2016). As a result, the Arctic terrestrial environment was  
70 significantly different from today, with boreal ecosystems at much higher latitudes (Salzmann et al., 2008). These  
71 changes in vegetation due to climate, may have also provided further important feedbacks to arctic temperatures (e.g.  
72 Otto-Bliesner and Upchurch Jr, 1997).

73 To advance our understanding of arctic ecosystem response and feedback to temperature amplification during past  
74 warm intervals in Earth's history this investigation targets an exceptionally well-preserved arctic sedimentary  
75 sequence to simultaneously reconstruct summer temperature, vegetation and fire from a single site.

## 76 2 Methods

### 77 2.1 Site description

78 To investigate the environment and climate of the Pliocene Arctic we focused on the Beaver Pond (BP) fossil site,  
79 located at 78° 33' N (Fig. 2) on Ellesmere Island. The stratigraphic section located at ~380 meters above sea level  
80 (MASL) today includes unconsolidated bedded sands and gravels, and rich organic layers including a fossil rich peat

Deleted: the latest ensemble of

Deleted: often under-predict the amplification of arctic temperatures during past warm intervals in Earth's history, including the Eocene (33.9–56 Ma; Shellito et al., 2009), and

Deleted: Ma; Dowsett et al., 2012; Salzmann et al., 2013) epochs.

Deleted: se

Deleted: differences

Deleted: either the models are not simulating the full array of feedback mechanisms properly for past climates, or that

Deleted: full

Deleted: If the later, the Arctic region and its ecosystems have yet to reach a new equilibrium in response to full temperature amplification.

Deleted: may

Deleted: .

96 layer, up to 2.4 m thick, with sticks gnawed by an extinct beaver (*Dipoides spp.*). The assemblage of fossil plants and  
97 animals at BP has been studied extensively to gain insight into the past climate and ecology of the Canadian High  
98 Arctic (Ballantyne et al., 2006; Csank et al., 2011a; Csank et al., 2011b; Fletcher et al., 2017; Mitchell et al., 2016;  
99 Rybczynski et al., 2013; Tedford and Harington, 2003; Wang et al., 2017). Previous paleoenvironmental evidence  
100 suggests the main peat unit is a rich fen deposit with a neutral to alkaline pH, associated with open water (Mitchell et  
101 al., 2016), likely a lake edge fen or shallow lake fen, within a larch-dominated forest-tundra environment (Matthews  
102 and Fyles, 2000), not a low pH peat-bog. While the larch species identified at the site, *Larix groenlandia*, is extinct  
103 (Matthews and Fyles, 2000), many other plant remains are Pliocene examples of taxa that are extant (Fletcher et al.,  
104 2017).

105 The fen-peat unit examined in this study was sampled in 2006 and 2010. The main sequence examined across the  
106 methods used in this study includes material from Unit II, the entire span of Unit III, and material from Unit IV  
107 sampled from Section A as per Mitchell et al. (2016; Fig. S1; see Mitchell et al. 2016 Fig 5), with a total sampled  
108 profile of 1.65 m. Unit III has been estimated to represent ~20 000 years of deposition based on modern northern fen  
109 accumulation rates (Mitchell et al., 2016). The charcoal [counts and measurements](#) from this locality were based on 31  
110 sample layers from the 2006 field campaign, while the temperature estimates from specific bacterial membrane lipids  
111 were taken from 22 of the sample layers collected in 2006 and an additional 12 samples collected in 2010. The same  
112 samples from the 2006 season were analyzed for mean summer temperature and char count where contents of the  
113 sample allowed. Pollen was tabulated from 10 samples from the 2006 sequence, located at different stratigraphic  
114 depths.

Deleted: estimates

## 115 2.2 Geochronology

116 While direct dating of the peat was not possible, we were able to establish a burial age for fluvial sediments deposited  
117 approximately 4–5 m above and 30 m to the southwest of the peat. We used a method based on the ratio of isotopes  
118 produced in quartz by secondary cosmic rays. The cosmogenic nuclide burial dating approach measures the ratio of  
119 cosmogenic  $^{26}\text{Al}$  ( $t_{1/2} = 0.71$  Ma) and  $^{10}\text{Be}$  ( $t_{1/2} = 1.38$  Ma) in quartz sand grains that were exposed on hillslopes and  
120 alluvium prior to final deposition at BP. Once the quartz grains are completely shielded from cosmic rays, the ratio of  
121 the pair will predictably decrease because  $^{26}\text{Al}$  has double the radiodecay rate of  $^{10}\text{Be}$ . In 2008, four of the medium to  
122 coarse grained quartz samples were collected from a vertical profile of planar crossbedded fluvial sands between 8.7  
123 and 10.4 m below the overlying till surface. The samples were 5 cm thick, separated by an average of 62 cm, and  
124 should closely date the peat (the sandy braided stream beds represent on the order of  $\sim 10^4$  years from the top of the  
125 peat to the highest sample). Quartz concentrates were extracted from the arkosic sediment using Frantz magnetic  
126 separation, heavy liquids, and differential leaching with HF in ultrasonic baths. When sample aliquots reached  
127 aluminum concentrations  $<100$  ppm (ICP-OES) as a proxy of feldspar abundance, the quartz concentrate was  
128 subjected to a series of HF digestion and rinsing steps to ensure that more than 30% of the quartz had been dissolved  
129 to remove meteoric  $^{10}\text{Be}$ . Approximately 200 mg of Be extracted from a Homestake Gold Mine beryl-based carrier  
130 was added to 150 g of each quartz concentrate (no Al carrier was needed for these samples). Such large quartz masses  
131 were digested because of the uncertainty in the abundance of the faster decaying isotope. Following repeated

133 perchloric-acid dry-downs to remove unreacted HF, pH-controlled precipitation, column chemistry ion  
134 chromatography to extract the Be and Al ions, precipitation in ultrapure ammonia gas, and calcination at temperatures  
135 above 1000°C in a Bunsen flame for three minutes, oxides were mixed with equal amounts of niobium and silver by  
136 volume. These were packed into stainless steel targets for measurement at Lawrence Livermore National Laboratory's  
137 accelerator mass spectrometer (AMS). Uncertainty estimates for  $^{26}\text{Al}/^{10}\text{Be}$  were calculated as  $1\sigma$  by combining AMS  
138 precision with geochemistry errors in quadrature. For a complete detailed description of TCN methods see Rybczynski  
139 et al. (2013). The ages provided here are updated from Rybczynski et al. (2013) by using more recent production rate  
140 information and considering the potential for increasing exposure to deeply penetrating muons during the natural post-  
141 burial exhumation at BP.

### 142 2.3 Paleotemperature Reconstruction

143 Paleotemperature estimates were determined based on the distribution of fossilized, sedimentary membrane lipids  
144 known as branched glycerol dialkyl glycerol tetraethers (brGDGTs) that are well preserved in peat bogs, soils, and  
145 lakes (Powers et al., 2004; Weijers et al., 2007c). These unique lipids are thought to be synthesized by a wide array of  
146 Acidobacteria within the soil (Sinninghe Damsté et al., 2011; Sinninghe Damsté et al., 2014) and presumably other  
147 bacteria (Sinninghe Damsté et al., 2018) in soils and peat bogs but also in aquatic systems. Previously, it has been  
148 established that the degree of methyl branching (expressed in the methylation index of branched tetraethers; MBT) is  
149 correlated with mean annual air temperature (MAAT), and the relative amount of cyclopentane moieties (expressed  
150 in the cyclization index of branched tetraethers; CBT) has been shown to correlate with both soil pH and MAAT  
151 (Weijers et al., 2007b). Because of the relationship of the distribution of these fossilized membrane lipids with these  
152 environmental parameters, [the distribution of these membrane lipids](#) has been used for paleoclimate applications in  
153 different environments including coastal marine sediments (Bendle et al., 2010; Weijers et al., 2007a), peats  
154 (Ballantyne et al., 2010; Naafs et al., 2017), paleosols (Peterse et al., 2011; Zech et al., 2012), and lacustrine sediments  
155 (Loomis et al., 2012; Niemann et al., 2012; Pearson et al., 2011; Zink et al., 2010). In this study we reconstruct mean  
156 summer air temperature (MST), using a modified version of a calibration that was developed by Pearson et al. (2011)  
157 and is based on 90 core top lacustrine sediment samples from diverse climates and geographical areas.

158 Improved separation methods (Hopmans et al., 2016) have recently led to the separation and quantification of the 5-  
159 and 6-methyl brGDGT isomers that used to be treated as one since the 6-methyl isomers were co-eluting with the 5-  
160 methyl isomers (De Jonge et al., 2013). This has led to the definition of new indices and improved MAAT calibrations  
161 based on the global soil (De Jonge et al., 2014), peat (Naafs et al., 2017), and African lake (Russell et al., 2018)  
162 datasets.

163 Sediment samples were freeze-dried and then ground and homogenized with a mortar and pestle. Next, using the  
164 Dionex™ accelerated solvent extractor (ASE), 0.5–1.0 g of sediment was extracted with the solvent mixture of  
165 dichloromethane (DCM):methanol (9:1, v/v) at a temperature of 100°C and a pressure of 1500 psi (5 min each) with  
166 60% flush and purge 60 s. The Caliper Turbovap®LV was utilized to concentrate the collected extract, which was  
167 then transferred using DCM and dried over anhydrous  $\text{Na}_2\text{SO}_4$  before being concentrated again under a gentle stream  
168 of  $\text{N}_2$  gas. To quantify the amount of GDGTs, 1  $\mu\text{g}$  of an internal standard (C46 GDGT; Huguet et al., 2006) was

Deleted: it



170 added to the total lipid extract. Then, the total lipid extract was separated into three fractions using hexane:DCM (9:1,  
 171 v:v) for the apolar fraction, hexane:DCM (1:1, v:v) for the ketone fraction and DCM:MeOH (1:1, v:v) for the polar  
 172 fraction, using a column composed of Al<sub>2</sub>O<sub>3</sub>, which was activated for 2 h at 150°C. The polar fraction, which contained  
 173 the GDGTs, was dried under a steady stream of N<sub>2</sub> gas and weighed before being re-dissolved in hexane:isopropanol  
 174 (99:1, v:v) at a concentration of 10 mg ml<sup>-1</sup> and subsequently passed through a 0.45 µm PTFE filter. Finally, the polar  
 175 fractions were analyzed for GDGTs by ultra-high performance liquid chromatography – atmospheric pressure positive  
 176 ion chemical ionization – mass spectrometry (UHPLC-APCI-MS) using the method described by Hopmans et al.,  
 177 (2016). The polar fractions of some samples were re-run on the UHPLC-APCI-MS multiple times and the average  
 178 fractional abundances of the brGDGTs was determined.

179 For the calculation of brGDGT-based proxies, the brGDGTs are specified by the Roman numerals as indicated in  
 180 Fig. S2. The 6-methyl brGDGTs are distinguished from the 5-methyl brGDGTs by a prime. The novel indices,  
 181 including MBT'<sub>5Me</sub> based on just the 5-methyl brGDGTs and the CBT' that was used to calculate the pH (De Jonge et  
 182 al., 2014):

$$183$$

$$184 \text{MBT}'_{5\text{Me}} = ([\text{Ia}] + [\text{Ib}] + [\text{Ic}]) / ([\text{Ia}] + [\text{Ib}] + [\text{Ic}] + [\text{IIa}] + [\text{IIb}] + [\text{IIc}] + [\text{IIIa}] + [\text{IIIb}] + [\text{IIIc}]) \quad (1)$$

$$185 \text{CBT}' = -^{10}\log\left(\frac{([\text{Ic}] + [\text{IIa}'] + [\text{IIb}'] + [\text{IIc}'] + [\text{IIIa}'] + [\text{IIIb}'] + [\text{IIIc}'])}{([\text{Ia}] + [\text{IIa}])}\right) \quad (2)$$

186

187 The square brackets denote the fractional abundance of the brGDGT within the bracket relative to the total brGDGTs.  
 188 The distributions of aquatically produced brGDGTs in the lake calibration developed by Pearson et al. (2011) were  
 189 used to determine MST. When this calibration is used the fractional abundances of IIa and IIa' must be summed  
 190 because these two isomers co-eluted under the chromatographic conditions used by Pearson et al. (2011):

$$191$$

$$192 \text{MST} (\text{°C}) = 20.9 + 98.1 \times [\text{Ib}] - 12 \times ([\text{IIa}] + [\text{IIa}']) - 20.5 \times [\text{IIIa}] \quad \text{RMSE} = 2.0\text{°C} \quad (3)$$

193

194 MAAT and surface water pH were also calculated using a novel calibration created using sediments from East African  
 195 lakes analysed with the novel chromatography method and based upon MBT'<sub>5Me</sub> (Russell et al., 2018).

$$196$$

$$197 \text{MAAT} = -1.2141 + 32.4223 * \text{MBT}'_{5\text{Me}} \quad \text{RMSE of } 2.44 \text{ °C} \quad (4)$$

$$198 \text{Surface water pH} = 8.95 + 2.65 * \text{CBT}' \quad \text{RMSE of } 0.80 \quad (5)$$

199 [Analytical error \(±0.38°C\) was estimated as the average standard deviation of the duplicates run on 18 of the samples](#)  
 200 [from throughout the section.](#)

Formatted: Line spacing: 1.5 lines

## 201 2.4 Vegetation and Fire Reconstruction

202 For charcoal, a total of thirty 2 cm<sup>3</sup> samples were taken at 5 cm intervals from depths from 380 and 381.45 MASL at  
 203 the BP site, with an additional 2cm<sup>3</sup> sample collected at 381.65 MASL. All samples were deflocculated using sodium  
 204 hexametaphosphate and passed through 500, 250 and 125 µm nested mesh sieves. The residual sample caught on each

205 sieve was then collected in a gridded petri dish and examined using a stereomicroscope at 20-40X magnification to  
206 obtain charcoal concentration (fragments cm<sup>-3</sup>). Charcoal area (mm<sup>2</sup> cm<sup>-3</sup>) was measured for each sample using  
207 specialized imaging software from Scion Corporation. For a detailed description of methods see Brown and Power  
208 (2013).

209 Vegetation was reconstructed using pollen and spores (herein pollen) at selected elevations chosen to capture upper  
210 and lower sections of the elevation profile, and that corresponded with changes in charcoal. The sample depths selected  
211 for pollen analyses were 380.3–380.4 MASL, 381.10–381.25 MASL, and 381.35–381.45 MASL. Samples were  
212 processed using standard approaches (Moore et al., 1991), whereby 1cm<sup>3</sup> sediment subsamples were treated with 5%  
213 KOH to remove humic acids and break up the samples. Carbonates were dissolved using 10% HCl, whereas silicates  
214 and organics were removed by HF and acetolysis treatment, respectively. Pollen slides were made by homogenizing  
215 35 µl of residue, measured using a single-channel pipette, with 15 µl of melted glycerin jelly. Slides were counted  
216 using a Leica DM4000 B LED compound microscope at 400–630x magnification. A reference collection and  
217 published keys (McAndrews et al., 1973; Moore et al., 1991) aided identification.

218 In addition to tabulating pollen and charcoal, a list of plant taxa derived from Beaver Pond was previously compiled  
219 in Fletcher et al. (2017). Extant species from this list were selected and their modern occurrences extracted from the  
220 Global Biodiversity Information Facility (GBIF.org, 2017). Observation data was grouped by 5° latitude 5° longitude  
221 grids cells, and the shared species count calculated using R (R Core Team, 2016). Modern fire frequency was mapped  
222 using the MODIS 6 Active Fire Product. The fire pixel detection count per day, within the same 5° latitude 5° longitude  
223 grids cells was tabulated over the ten years 2006–2015, and standardized by area of the cell. The modern climate maps  
224 were generated using data from WorldClim 1.4 (Hijmans et al., 2005). The values for the bioclimatic variables mean  
225 temperature of the warmest quarter (equivalent to MST) and precipitation of the warmest quarter (summer  
226 precipitation) were also averaged by grid cell. The shared species count, climate values, and fire day detections were  
227 mapped to the northern polar stereographic projection in ArcMap 10.1.

Formatted: Not Superscript/ Subscript

Deleted: counted

## 228 3 Results

### 229 3.1 Geochronology

230 The burial dating results with <sup>26</sup>Al/<sup>10</sup>Be in quartz sand at 10 m below modern depth provides four individual ages.  
231 From shallowest to deepest, the burial ages are 3.6 +1.5/-0.5 Ma, 3.9 +3.7/-0.5 Ma, 4.1 +5.8/-0.4 Ma, and 4.0 +1.5/-  
232 0.4 Ma (Table S2), with an unweighted mean age of 3.9 Ma. The convoluted probability distribution function yields  
233 a maximum probability age of 4.5 Ma. Unfortunately, the positive tails of the probability distribution functions of two  
234 of the samples exceeds the radiodecay saturation limit of the burial age. Therefore, their probability distributions do  
235 not reflect the actual age probabilities and uncertainty. Given the positive tail in the probability distribution functions,  
236 and the inability to convolve all samples, we recommend using the unweighted mean age, 3.9 Ma, with an uncertainty  
237 of +1.5/-0.5 Ma as indicated by the two samples with unsaturated limits. Despite the apparent upward younging of the  
238 individual burial ages, the 1σ-uncertainties overlap rendering the samples indistinguishable.

## 240 3.2 Paleotemperature Estimates

### 241 3.2.1 Provenance of branched GDGTs

242 Previously, brGDGT derived MAAT estimates ( $-0.6 \pm 5.0$  °C) from BP sediments were developed using the older  
243 chromatography methods that did not separate the 5- and 6- methyl brGDGTs, and a soil calibration (Ballantyne et  
244 al., 2010). In marine and lacustrine sediments, bacterial brGDGTs were thought to originate predominantly from  
245 continental soil erosion arriving in the sediments through terrestrial runoff. More recent studies, however, have  
246 indicated aquatically produced brGDGTs could be affecting the distribution of the sedimentary brGDGTs and thus  
247 the temperature estimates based upon them (Warden et al., 2016; Zell et al., 2013; Zhu et al., 2011). Since the discovery  
248 that sedimentary brGDGTs can have varying sources, different calibrations have been developed depending on the  
249 origin of the brGDGTs, i.e. soil calibration (De Jonge et al., 2014), peat calibration (Naafs et al., 2017) and aquatic  
250 calibrations (i.e. Foster et al., 2016; Pearson et al., 2011; Russell et al., 2018). Therefore, several studies have  
251 recommended that the potential sources of the sedimentary brGDGTs should be investigated before attempting to use  
252 brGDGTs for paleoclimate applications (De Jonge et al., 2015; Warden et al., 2016; Yang et al., 2013; Zell et al.,  
253 2013). In this study, we examine the distribution of brGDGTs in an attempt to determine their origin and consequently  
254 the most appropriate calibration to utilize in order to reconstruct temperatures from the BP sediments.

255 Branched GDGTs IIIa and IIIa' on average had the highest fractional abundance of the brGDGTs detected in the BP  
256 sediments (see Fig. S2 for structures; Table S4). A previous study established that when plotted in a ternary diagram  
257 the fractional abundances of the tetra-, penta- and hexamethylated brGDGTs, soils lie within a distinct area (Sinninghe  
258 Damsté, 2016). To assess whether the brGDGTs in the BP deposit were predominantly derived from soils, we  
259 compared the fractional abundances of the tetra-, penta- and hexamethylated brGDGTs in the BP sediments to those  
260 from modern datasets in a ternary diagram (Fig. 3). Since the contribution of brGDGTs from either peat or aquatic  
261 production could affect the use of brGDGTs for paleoclimate application, in addition to comparing the samples to the  
262 global soil dataset (De Jonge et al., 2014), peat and lacustrine sediment samples were added into the ternary plot to  
263 help elucidate the provenance of brGDGTs in the BP sediments. According to Sinninghe Damsté (2016), it is  
264 imperative to only compare samples in a ternary diagram like this where all of the datasets were analyzed with the  
265 novel methods that separate the 5- and 6-methyl brGDGTs since the improved separation can result in an increased  
266 quantification of hexamethylated brGDGTs. Recently, samples from East African lake sediments were analyzed using  
267 these new methods (Russell et al., 2018) and so these samples were included in the ternary plot for comparison (Fig.  
268 3). Although the lakes from the East African dataset are all from a tropical area, they vary widely in altitude and, thus,  
269 in MAAT. We separated them into three categories by MAAT (lakes  $>20$ °C, lakes between  $10$ - $20$ °C and lakes  $<10$ °C).  
270 By comparing all the samples in the ternary plot, it was evident that the BP samples plotted closest to the lacustrine  
271 sediment samples from regions in East Africa with a MAAT  $<10$ °C, suggesting that the provenance of the majority  
272 of the brGDGTs from the BP sediments was not soil or peat but lacustrine aquatic production.

273 The average estimated surface water pH for the BP sediments ( $8.6 \pm 0.2$ ) calculated using eq. (5), is within the 6 –9  
274 range typical of lakes and rivers (Mattson, 1999). This value is near the upper limit of rich fens characterized by the  
275 presence of *S. scorpioides* (Kooijman and Westhoff, 1995; Kooijman and Paulissen, 2006) and is higher than what  
276 would be expected for peat-bog sediments that are acidic (pH 3–6; Clymo, 1964) and which constitute most of the

277 peats studied by Naafs et al. (2017). A predominant origin from lake aquatic production is in keeping with previous  
278 interpretation of the paleoenvironment of the BP site, which was at least at times covered by water as evidenced by  
279 fresh water diatoms, fish remains and gnawed beaver sticks in the sediment (Mitchell et al., 2016).

### 280 3.2.2 Aquatic Temperature Transfer Function

281 Since there is evidence that the majority of the brGDGTs in the BP sediments are aquatically produced, an aquatic  
282 transfer function was used for reconstructing temperature. When we apply the African lake calibration (Eq. 4), the  
283 resulting estimated MAAT for BP is  $7.1 \pm 1.0$  °C (mean  $\pm$  standard deviation). This value is high compared to other  
284 previously published estimates from varying proxies, which have estimated MAAT in this region to be in the range  
285 of -5.5 to 0.8°C, (Ballantyne et al., 2010; Ballantyne et al., 2006; Csank et al., 2011a; Csank et al., 2011b; Fletcher et  
286 al., 2017). A concern when applying this calibration is that it is based on lakes from an equatorial region that does not  
287 experience substantial seasonality, whereas, the Pliocene Arctic BP site did experience substantial seasonality  
288 (Fletcher et al., 2017). Biological production (including brGDGT production) in BP was likely skewed towards  
289 summer and, therefore, summer temperature has a larger influence on the reconstructed MAAT. Unfortunately, no  
290 global lake calibration set using individually quantified 5- and 6-methyl brGDGTs is yet available. Therefore, to  
291 calculate MST (Eq. 3) we applied the aquatic transfer function developed by Pearson et al. (2011) by combining the  
292 individual fractional abundances of the 5- and 6-methyl brGDGTs. The Pearson et al. (2011) calibration was based on  
293 a global suite of lake sediments including samples from the Arctic, thus covering a greater range of seasonal  
294 variability. The resulting average estimated MST was  $15.4 \pm 0.8$  °C (mean  $\pm$  1 standard deviation, n = 34 samples),  
295 with temperatures ranging between 14.1 and 17.4 °C (Fig. 4). This is in good agreement with recent estimates based  
296 on Climate Reconstruction Analysis using Coexistence Likelihood Estimation (CRACLE; Fletcher et al., 2017) that  
297 concluded that MSTs at BP during the Pliocene were approximately 13 to 15°C.

Deleted: average

### 298 3.3 Vegetation and Fire Reconstruction

299 All sediment samples from BP contained charcoal (Fig. 4), indicating the consistent prevalence of biomass burning in  
300 the High Arctic during this time period. However, counts were variable throughout the section, with the middle and  
301 lower sections (mean 34 fragments cm<sup>-3</sup>) containing less charcoal compared to the upper section upper section (mean  
302 444 fragments cm<sup>-3</sup>). Overall, samples from BP contained on average  $100.0 \pm 165$  fragments cm<sup>-3</sup> (mean  $\pm$  1  $\sigma$ ), with  
303 charcoal area averaging  $12.3 \pm 20.2$  mm<sup>2</sup> cm<sup>-3</sup>. The variability of charcoal within any given sample was relatively low  
304 with a 1  $\sigma$  among charcoal area of approximately 2 mm<sup>2</sup> cm<sup>-3</sup>.

305 The three parts of the section analysed for pollen (380.3–380.4 MASL, 381.15–381.25 MASL, and 381.35–381.45  
306 MASL) reveal variations in vegetation (Figs. 4 and 5). Near the bottom of the section (380.3-380.4 MASL), *Larix*  
307 (26%) and *Betula* (17%) were the dominant trees. *Alnus* (6%) and *Salix* (6%) together with ericaceous pollen (4%)  
308 were relatively high. In contrast, low numbers of *Picea* (3%), *Pinus* (3%) and fern spores were recorded. Additional  
309 wetland taxa like *Myrica* (5%) and Cyperaceae (6%) were also noted. Overall, the non-arboreal (23%) signal was well  
310 developed. Crumpled and/or ruptured inaperturate grains with surface sculpturing that varied from scabrate to  
311 verrucate were noted in the assemblage (12%), but could not be definitively identified. It is possible that these grains

Deleted: ely

314 represent *Populus*, Cupressaceae or additional Cyperaceae pollen. Between 381.10-381.25 MASL, *Larix* (38%) and  
315 *Betula* (21%) increased in abundance, followed by ferns (7%). Cyperaceae remained at similar levels (6%) whereas  
316 *Picea* and *Pinus* decreased to 2% and 1%, respectively. Unidentified inaperturate types collectively averaged 14%.  
317 *Larix* pollen (23%) remained abundant near the top of the section (381.35-381.45 MASL), whereas *Betula* (2%)  
318 decreased. *Picea* (16%) *Pinus* (6%) and ferns (23%) increased in abundance. Of the ferns, trilete spores and cf.  
319 *Botrychium* were most abundant, followed by cf. *Dryopteris*. Inaperturate unknowns (10%) were also observed. Other  
320 notables included Ericaceae (2%) and Cyperaceae (2%). While rare, Onagraceae grains were also observed (Fig. 5).

321 According to the GBIF-based mapping exercise, the paleofloral assemblage at BP most closely resembles modern  
322 vegetation found in northern North America, particularly on the eastern margin (e.g. New Hampshire, New Brunswick  
323 and Nova Scotia) and the western margin (Alaska, Washington, British Columbia, and Alberta; Fig. 7a), and central  
324 Fennoscandia. Of these areas, the western coast of northern North America and eastern coast of southern Sweden have  
325 the most similarity to the reconstructed BP climate in terms of MST (Fig. 7b) and summer precipitation (Fig. 7c).

326 While high counts of active fire days are common in the western part of the North American boreal forest, it is not  
327 as common in the eastern part of the North American boreal forest (Fig. 7d), likely due to the differences in the  
328 precipitation regime. Low fire counts also typified Fennoscandia, likely due to historical severe fire suppression  
329 (Brown and Giesecke, 2014; Niklasson and Granström, 2004). Therefore, based on our reconstruction of the climate  
330 and ecology of the BP site, our results suggest that BP most closely resembled a boreal-type forest ecosystem shaped  
331 by fire, similar to those of Washington, British Columbia, Northwest Territories, Yukon and Alaska (Figure 3; but see  
332 Sect. 4.3).

## 333 4 DISCUSSION

### 334 4.1 Geochronology

335 The plant and animal fossil assemblages observed at BP suggest a depositional age between 3 and 5 Ma (Matthews Jr  
336 and Ovensen, 1990; Tedford and Harington, 2003). This biostratigraphic age was corroborated with an amino-acid  
337 racemization age ( $>2.4 \pm 0.5$  Ma) and Sr-correlation age (2.8–5.1 Ma) on shells (Brigham-Grette and Carter, 1992) in  
338 biostratigraphically correlated sediments on Meighen Island, situated 375 km to the west-north-west. The previously  
339 calculated burial age of 3.4 Ma for the BP site is a minimum age because no post-depositional production of  $^{26}\text{Al}$  or  
340  $^{10}\text{Be}$  by muons was assumed. If the samples are considered to have been buried at only the current depth (ca. 10 m,  
341 see supplemental data) then the ages plot to the left and outside of the burial field, indicating that the burial depth was  
342 significantly deeper for most of the post-depositional history. The revised cosmogenic nuclide burial age is  $3.9 + 1.5/-$   
343  $0.5$  Ma. It is the best interpretation of burial age data based on improved production rate systematics (e.g. Lifton et  
344 al., 2014), and more reasonable estimates of erosion rate and ice cover since the mid-Pliocene (see Fig. S3; Table S5).  
345 As the stratigraphic position of the cosmogenic samples is very close to the BP peat layers, we interpret the age to  
346 represent the approximate time that the peat was deposited.

Deleted: s

Deleted: There were also 1

Deleted: in

350 **4.2 Fire, vegetation, temperature: a feedback triangle**

351 Wildfire is a key driver of ecological processes in modern boreal forests (Flannigan et al., 2009; Ryan, 2002), and  
352 although historically rare, is becoming more frequent in the tundra in recent years (Mack et al., 2011). The modern  
353 increase in fire frequency is likely as a consequence of atmospheric CO<sub>2</sub> driven climate warming and feedbacks such  
354 as reduced sea ice extent (Hu et al., 2010), because the probability of fire is highest where temperature and moisture  
355 are conducive to growth and drying of fuels followed by conditions that favor ignition (Whitman et al., 2015). Young  
356 et al. (2017) confirmed the importance of summer warmth and moisture availability patterns in predicting fire across  
357 Alaska, highlighting a July temperature of ~13.5 °C as a key threshold for fire across Alaska.

358 The abundance of charcoal at BP demonstrates that climatic conditions were conducive to ignition and that sufficient  
359 biomass available for combustion existed across the landscape. brGDGTs-derived temperature estimates suggest mean  
360 summer temperatures at BP exceeded the ~13.5 °C threshold (Young et al., 2017) that drastically increases the chance  
361 of wildfire. Indeed, the estimate of ~15.4°C suggests mean reconstructed summer temperatures were ~11°C higher  
362 than modern day Eureka, Canada (~4.1°C; Fig. 2) representing substantial additional amplification compared to the  
363 global average. Without the increased arctic amplification of temperature that accompanies climate equilibrium with  
364 high CO<sub>2</sub>, mean summer temperatures would be lower than the July temperature threshold that predicts increased  
365 wildfire. This is evidence that Pliocene arctic amplification of temperatures was a direct feedback to increased wildfire  
366 activity. The increased extent of boreal forest into the Arctic was also possible due to arctic amplification of  
367 temperatures. This biomass provided the fuel for combustion and thus Pliocene arctic amplification of temperatures  
368 is also an indirect feedback to wildfire (Fig. 6).

369 Conversely, the charcoal record at BP suggests substantial biomass burning that could have acted as a feedback  
370 mechanism amplifying or dampening warming seasonally during the mid-Pliocene (Fig. 6). Studies of the impact of  
371 wildfire on surface energy balance in present-day northern ecosystems have revealed the complexity of predicting  
372 wildfire's impact on climate. Ecosystems exhibit changing responses through time from the scale of years post-burning  
373 (Randerson et al. 2006; Bonan, 2008; French et al. 2016), to seasonal (Huang et al., 2015), and even diurnal differences  
374 post-deforestation that may impact net wildfire feedback to climate (Shultz et al., 2017). The radiative response to  
375 wildfire changes across latitudinal gradients (Jin et al., 2012), and between local and global scales (Ward et al., 2012;  
376 Liu et al., 2019). Additionally, the original vegetation type burned influences aspects of wildfire's impact on climate  
377 such as the original albedo (French et al., 2016), likely fire severity and intensity (Rogers et al 2015), and time to pre-  
378 fire ecosystem recovery (French et al., 2016) or alternate ecosystem establishment (Johnstone et al., 2010b). The  
379 mechanisms that appear to have the largest effect include carbon release and sequestration (e.g. Harrison et al. 2018),  
380 changes in surface albedo (e.g. Huang et al. 2015), altered evapotranspiration (Liu et al 2019), and aerosol effects both  
381 directly and also indirectly via cloud processes (e.g. Stone et al., 2008; Zhang et al., 2017). Wildfires' potential role as  
382 a feedback to climate in the mi-Pliocene Arctic is suggested by its prevalence through this >20000 year sequence, the  
383 impact of forest fire in modern ecosystems, and preliminary modelling of the complex direct impacts on the surface  
384 radiative budget (e.g. short term black carbon deposition on snow and ice and long-term changes in albedo) and direct  
385 and indirect effects on the top of the atmosphere radiative budget (i.e. aerosol emissions; Feng et al., 2016). Further

Deleted: is

Deleted: Given a global mean increase of 3°C for the Pliocene compared to modern (see fig. 1) this 11°C increase represents 3.6x arctic amplification of temperature (NB. although comparing summer temperatures to mean global temperature increase is likely imprecise, given much increase of arctic warmth in Pliocene climate models is from winter warming (see Ballantyne et al. 2013) 3.6x is likely an underestimate rather than an overestimate.)

Deleted: ing

Deleted: ies increasing

Deleted: fall below

Deleted:

Deleted: ~13.5°C

Deleted: ,

Deleted: but also

Deleted: as the increased extent of boreal forest into the higher latitudes, also possible due to arctic amplification of temperatures, provided the fuel (Fig. 6)

Moved (insertion) [1]

Deleted:

Deleted: Its

Deleted: time

Deleted: forest fire's

408 [modelling experiments are needed to determine if wildfire played a significant role in the magnitude and seasonal](#)  
409 [patterns of mid-Pliocene arctic amplification of temperature.](#)

410 An increase in atmospheric convection has been simulated in response to diminished sea-ice during warmer intervals  
411 (Abbot and Tziperman, 2008), but this study did not confirm if this increase in atmospheric convection was sufficient  
412 to cause lightning ignitions. An alternative ignition source for combustion of biomass on Ellesmere Island during the  
413 Pliocene is coal seam fires, which have been documented to be burning at this time (Estrada et al., 2009). However,  
414 given the interaction of summer warmth and ignition by lightning within the same climate range as posited for BP, we  
415 consider lightning the most likely source of ignition for Pliocene fires in the High Arctic.

416 Fire return intervals cannot be calculated from the BP charcoal counts due to the absence of a satisfactory age-depth  
417 model and discontinuous sampling. As strong interactions are observed between fire regime and ecosystem  
418 assemblage in the boreal forest (Brown and Giesecke, 2014; Kasischke and Turetsky, 2006), and in response to  
419 climate, comparison with modern fire regimes for areas with shared species compositions and climates may inform a  
420 potential range of mean fire return interval (MFR).

421 Matthews and Fyles (2000) indicated that the Pliocene BP environment was characterized by an open larch  
422 dominated forest-tundra environment, sharing most species in common with those now found in three regions,  
423 including central Alaska to Washington in western North America, the region centered around the Canadian/US border  
424 in eastern North America, as well as Fennoscandia in Europe. The modern area with the most species in common with  
425 BP is central northern Alaska (Fig. 7A). The area over which shared species were calculated is largely tundra, but  
426 includes the ecotone between tundra and boreal forest. Other zones that share many species with BP are continuous  
427 with Alaska down the western coast of North America to the region around the border of Canada and the United States,  
428 the eastern coast of North America in the region around the border of Canada and the United States (~50°N), and  
429 central Fennoscandia. Of these zones, the MST of Alaskan tundra sites (6–9°C) are less similar to BP (15.4°C) than  
430 ~50°N on both western and eastern coastal North American sites and central Fennoscandia (12–18°C, Fig. 7B). The  
431 eastern coast of North America has higher rainfall during the summer (>270 mm), than the west coast and Alaska  
432 (Fig. 7C), which correlates to the timing of western fires. The low summer precipitation for much of the west (<200  
433 mm), is consistent with previously published summer precipitation estimates for BP (~190 mm). As a result, the fire  
434 regime of the west coast ~50°N may be a better analogue for BP than the east coast of North America. In central  
435 Fennoscandia there is also a west vs. east coastal variation in summer precipitation with the western, Nordic part of  
436 the region experiencing higher summer precipitation (252– >288 mm), than the more similar eastern, Swedish part of  
437 the region (~198 mm).

438 Investigation of the modern fire detection data (Fig. 7D) suggests that the two regions most climatically similar to  
439 BP, ~50°N western North America and central Sweden, have radically different fire regimes. It is likely this is caused  
440 by historical fire suppression in Sweden that limits the utility of modern data for comparison with this study (Brown  
441 and Giesecke, 2014; Niklasson and Granström, 2004). To understand the fire regimes, as shaped by climate and species  
442 composition rather than human impacts, we considered both the modern and recent Holocene reconstructions for these  
443 regions (Table 1). This shows that, a) within any region variation arises from the complex spatial patterning of fire  
444 across landscapes, and b) that the regions most similar to BP (~50°N western North American and eastern

445 Fennoscandian reconstructions for the recent Holocene) have shorter fire return intervals than the cooler Alaskan  
446 tundra or wetter summer ~50°N region of the eastern North American coast.

447 While the shared species for Siberia appears low, the [total](#) number of observations [for Siberia](#) in the modern  
448 biodiversity database used is likewise low – ~~and the latter is a potential cause of the former~~. Given the similar climate  
449 to BP on the Central Siberian Plateau and some key aspects of the floras in Siberia such as the dominance of larch,  
450 we considered the fire regime of the larch forests of Siberia. Kharuk et al. (2016; 2011) studied MFRI across Siberia,  
451 from 64°N to 71°N, the northern limit of larch stands. They found an average MFRI across that range of 110 years,  
452 with MFRI increasing from 80 years in the southern latitudes to ~300 in the north (Table 1). Based on similarity of  
453 the climate variables, the more southerly MFRI (~80 years) may be a better analogue. Key differences between boreal  
454 fires in North America compared to Russia are a higher fire frequency with more burned area in Russia, but a much  
455 lower crown fire and a difference in timing of disturbance, with spring fires prevailing in Russia compared to mid-  
456 summer fires in western Canada (de Groot et al., 2013; Rogers et al., 2015).

457 The pollen-based vegetation reconstruction derived in this study indicates that open *Larix-Betula* parkland persisted  
458 in the basal (380.3-380.4 MASL) parts of the sequence. Groundcover was additionally dominated by shrub birch,  
459 ericaceous heath and ferns. While the regional climate may have been somewhat dry, the record suggests that, locally,  
460 a moist fen environment dominated by Cyperaceae, existed near the sampling location. Shrubs including *Alnus* and  
461 *Salix* likely occupied the wetland margins.

462 The corresponding relatively low concentration of charcoal [in this stratigraphic interval](#) may reflect lower severity  
463 fires or higher sedimentation rates. We consider the former more likely due to the depositional environment of Unit  
464 III from Mitchell et al. 2016, a lake edge fen peat in a beaver pond or small lake, without evidence of high sediment  
465 influx overwhelming peat production. We posit that a surface fire regime, somewhat like that in southern central  
466 Siberia existed. This premise is also supported by the fire ecology characteristics of the dominant vegetation. *Larix*  
467 does not support crown fires due to leaf moisture content (de Groot et al., 2013) and self-pruning (Kobayashi et al.,  
468 2007). The persistence and success of larch in modern-day Siberia appears to be driven by its high growth rate  
469 (Jacquelyn et al., 2017), tolerance of frequent surface fire due to thick lower bark (Kobayashi et al., 2007), and  
470 tolerance of spring drought due to its deciduous habit (Berg and Chapin III, 1994). Arboreal *Betula* are very intolerant  
471 of fire and easily girdled. However, they are quick to resprout and are often found in areas with short fire return  
472 intervals. Like *Larix*, arboreal *Betula* have high moisture content of their foliage and are not prone to crown fires.  
473 *Betula nana* L., an extant dwarf birch, is a fire endurer that resprouts from underground rhizomes or roots (Racine et  
474 al., 1987) thus regenerating quickly following lower severity fires (de Groot et al., 1997). The vegetation and fire  
475 regime characteristics are similar further up the sequence at 381.10-381.25 MASL, with the exception that ferns  
476 increased in abundance while heath decreased.

477 In the upper part of the sequence (381.35-381.45 MASL), where charcoal was abundant, the *Larix-Betula* parkland  
478 was replaced by a mixed boreal forest assemblage with a fern understory. Canopy cover was more closed compared  
479 to the preceding intervals. The forest was dominated by *Larix* and *Picea*, with lesser amounts of *Pinus*. While *Betula*  
480 remained part of the forest, it decreased in abundance possibly due to increased competition with the conifers. Based  
481 on exploratory CRACLE analyses of climate preferences using GBIF occurrence data (GBIF.org, 2018a, b, c, d) of

Deleted: perhaps causatively so



483 the dominant taxa (*Larix-Betula* vs. *Larix-Picea-Pinus*), the expansion of conifers could indicate slightly warmer  
484 summers (MST ~15.8 °C vs. 17.1 °C). This result differs from the stable MST estimated by bacterial tetraethers,  
485 although within reported error, and the small change is certainly within the climate distributions of both communities.  
486 The CRACLE analyses also suggest that slightly drier conditions may have prevailed during the three wettest months  
487 (249-285mm vs. 192-219mm). While the interaction between climate, vegetation and fire is complex, small changes  
488 in MST and precipitation could have directly altered both the vegetation and fire regime, which in turn further  
489 promoted fire adapted taxa. In addition to regional climatic factors, community change at the site may have been  
490 further influenced by local hydrological conditions, such as channel migration, pond infilling and ecosystem  
491 engineering by beaver (*Dipoides sp.*).

492 The high charcoal content of the upper portion (~ Unit IV) of the sequence has three potential explanations:  
493 reworking of previously deposited charcoal, decreased sedimentation, or increased wildfire production of charcoal.  
494 The first explanation seems unlikely because there is no difference in the shape of the macrocharcoal between the  
495 upper and lower portions of the sequence. A change in the dimensions of the charcoal would be expected if it had  
496 undergone additional physical breakdown from reworking (see Fig. S4). The second, decreased sedimentation, may  
497 occur if the deposition is a result of infrequent, episodic flooding intermixed with long periods during which charcoal  
498 was deposited. The recorded sedimentology does not support this explanation, but due to the complexity of flooding  
499 processes, also does not disprove this explanation. The third explanation, that increased charcoal reflects increased  
500 wildfire, is supported by the change in plant composition, and suggests that frequent, mixed severity fires may have  
501 persisted at this time. While *Larix* is associated with surface fire, *Picea* and *Pinus* are adapted to higher intensity  
502 crown fires. A crown fire regime may have established as conifers expanded, altering fuel loads and flammability. For  
503 example, black spruce sheds highly flammable needles, its lower branches can act as fuel ladders facilitating crown  
504 fires (Kasischke et al., 2008), and black spruce was previously tentatively identified at BP (Fletcher et al., 2017).  
505 While it has thin bark and shallow roots maladapted to survive fire (Auclair, 1985; Brown, 2008; Kasischke et al.,  
506 2008), it releases large numbers of seeds from semi-serotinous cones, leading to rapid re-establishment (Côté et al.,  
507 2003). The documentation of Onagraceae pollen at the top of the sequence could potentially reflect post-fire  
508 succession. For example, the species *Epilobium angustifolium* L. is an early-seral colonizer of disturbed (i.e. burned)  
509 sites, pollinated by insects.

510 It appears that the *Larix-Betula* parkland dominated intervals correspond to the peat- and sand-stratigraphic Units II  
511 and III described by Mitchell et al. (2016), whereas the mixed boreal forest in the upper part of the sequence is  
512 contemporaneous with Unit IV, described as peat and peaty sand, coarsening upwards. Thus, while vegetation and  
513 fire regimes seemingly changed through time at this Arctic site, temperatures appear more stable, or at least to have  
514 no apparent trend within analytical and reconstruction uncertainty. Thus, it is suggested that the fire regime at BP was  
515 primarily regulated by regional climate and vegetation, and perhaps additionally by changing local hydrological  
516 conditions. Regarding climate, MST remained high enough (> ~13.5°C) throughout the sequence to allow for fire  
517 disturbance and the pollen suggests that temperatures may have marginally increased in the upper part of the sequence.  
518 Alternatively, other climate variables, such as the precipitation regime, or local hydrological change may have initiated  
519 the change in vegetation community. Up-sequence changes in vegetation undoubtedly influenced fine fuel loads (e.g.

Deleted: *Cantor spp.*

Formatted: Font: Italic

Deleted: We consider the

Deleted: ,

Deleted: whereas we would anticipate a

Deleted: We, however, favour t

Deleted: of

Deleted: due to

Deleted: consistent with a greater influence of fire

Deleted: . If accepted, it is likely

Deleted: it

Deleted: While

Deleted: it is clear that the

532 [surface layer needles, mosses, and twigs](#)) and flammability. Indeed, the fire ecological characteristics of the vegetation  
533 are consistent with a regional surface fire regime yielding to a crown fire regime.

534 *Betula* and *Alnus*, which occurred earlier in the depositional sequence, are favored by beaver in foraging (Busher,  
535 1996; Haarberg and Rosell, 2006; Jenkins, 1979). Moreover, the presence of sticks cut by beaver in Unit III reveals  
536 that beavers were indeed at the site, moistening the local land surface. The lack of beaver cut sticks and changes in  
537 sediment in Unit IV may indicate that the beavers abandoned the site, possibly in response to changes in vegetation  
538 (i.e. increased conifers and decreased *Betula*) limiting preferred forage or due to lateral channel migration, as  
539 evidenced by the coarsening upward sequence described by Mitchell et al. (2016). As a result, the local land surface  
540 may have become somewhat drier, contemporaneous with the change towards *Larix-Picea-Pinus* forest and a mixed  
541 severity fire regime.

## 542 5. CONCLUSION

543 The novel temperature estimates presented here confirm that [Ellesmere Island](#) summer temperatures were  
544 considerably warmer ( $15.4 \pm 0.8$  °C) during the [likely >20000-year mid-Pliocene interval \(3.9 +1.5/-0.5 Ma\)](#)  
545 [investigated](#), compared to the modern Arctic. The  $\sim 11$ °C higher [than present day](#) summer temperatures at Beaver Pond  
546 support an increasing [effect](#) of arctic amplification of temperatures when CO<sub>2</sub> reaches and exceeds modern levels. Our  
547 reconstruction of the paleovegetation and ecology of this unique site on Ellesmere Island suggests an assemblage  
548 similar to forests of the western margins of North America and eastern Fennoscandia. The evidence of recurrent fire  
549 and concurrent changes in taxonomic composition are indicators that fire played an active role [in mid-Pliocene Arctic](#)  
550 forests, shaping the environment as it does in the boreal forest today. Evidence from fire in the modern boreal forest  
551 suggests that fire may have had direct and indirect impacts on Earth's radiative budget at high latitudes during the  
552 Pliocene, acting as a feedback to Pliocene climate. The net impact of the component process remains unknown and  
553 modelling experiments are needed to quantitatively investigate the effects of the kind of fire regime presented here,  
554 on the Pliocene High Arctic. Collectively, these reconstructions provide new insights into the paleoclimatology and  
555 paleoecology of the Canadian High Arctic,  $\sim 3.9$  Ma.

556  
557 *Data Availability.* The data generated and used in this analysis are available in the supplemental information associated  
558 with this article.

559  
560 *Sample Availability.* Samples used in this analysis are curated by the Canadian Museum of Nature. Sample numbers  
561 used for each analysis are given in the supplemental information (Table S3 and S4).

562  
563 *Supplemental Link.* To be provided by Copernicus Publishing

564  
565 *Author Contribution.* Conceptualization: A.P.B. with modification by other authors; Methodology: J.G., J.S.S.D.,  
566 K.J.B., T.F.; Formal analysis: All authors; Investigation: A.P.B., J.G., K.J.B., L.W., T.F.; Resources: A.P.B., J.G.,  
567 J.S.S.D., K.J.B.; Data curation: A.P.B., J.G., K.J.B., L.W., T.F.; Writing—Original draft: All authors; Writing—

**Moved up [1]:** the charcoal record at BP suggests substantial biomass burning that could have acted as a feedback mechanism amplifying or dampening warming during the Pliocene. Its potential role as a feedback to climate is suggested by its prevalence through time, and forest fire's complex direct impacts on the surface radiative budget (e.g. black carbon deposition on snow and ice) and direct and indirect effects on the top of the atmosphere radiative budget (i.e. aerosol emissions; Feng et al., 2016).

**Deleted:** [↑](#)  
- Critically,

**Deleted:** Further investigation through both investigation of the fire record at other Arctic sites and modelling experiments using varying fire regimes and extent is warranted to better characterize the fire regime in order to improve accuracy of fire simulations in earth system models of Pliocene climate.

**Deleted:** ( $15.4 \pm 0.8$  °C)

**Deleted:** influence

**Deleted:** as a feedback

586 Review and editing: All authors; Supervision: A.P.B., J.S.S.D., K.J.B., N.R.; Project administration: A.P.B., N.R.,  
587 T.F.; Funding acquisition: A.P.B., J.G., J.S.S.D., K.J.B., N.R., T.F. (Definitions as per the CRediT Taxonomy)

588

589 *Competing interests.* The authors declare that they have no conflict of interest

590

591 *Acknowledgements.* This work was funded by NSF Polar Programs to A.P.B.; National Geographic Committee for  
592 Research and Exploration Grant (9912-16) and Endeavour Research Fellowship (5928-2017) to T.F.; National  
593 Geographic Explorer Grant (7902-05), NSERC Discovery Grant (312193), and The W. Garfield Weston Foundation  
594 grant to N.R.; student travel (N.R. supervised) was supported by the Northern Scientific Training Program (NSTP)  
595 from the government of Canada; an NSERC Discovery Grant (239961) with Northern Supplement (362148) to J.C.G.;  
596 Natural Resources Canada (SO-03 PA 3.1 Forest Disturbances Wildland Fire) to K.J.B.; the European Research  
597 Council under the European Union's Seventh Framework Programme (FP7/2007-2013) / ERC grant agreement n°  
598 [226600](#), and funding from the Netherlands Earth System Science Center (NESSC) through a gravitation grant (NWO  
599 024.002.001) from the Dutch Ministry for Education, Culture and Science to J.S.S.D.

600 We are also grateful to Nicholas Conder (Canadian Forest Service) who assisted with sample preparation for the  
601 vegetation/fire reconstruction. We also acknowledge the 2006, 2008, 2010 and 2012 field teams including D. Finney  
602 (Environment Canada), H. Larson (McGill University), M. Vavrek (McGill University), A. Dececchi (McGill  
603 University), W.T. Mitchell (Carleton University), R. Smith (University of Saskatchewan), and C. Schröder-Adams  
604 (Carleton University). The field research was supported by a paleontology permit from the Government of Nunavut,  
605 CLEY (D.R. Stenton, J. Ross) and with the permission of Qikiqtani Inuit Association, especially Grise Fiord  
606 (Nunavut). Logistic support was provided by the Polar Continental Shelf Program (M. Bergmann, B. Hycryk, B.  
607 Hough, M. Kristjanson, T. McConaghy, J. MacGregor and the PCSP team) [and in-kind financial support through](#)  
608 [PCSP-616-16 was greatly appreciated.](#)

## 609 References

610 Abbot, D. S. and Tziperman, E.: Sea ice, high-latitude convection, and equable climates, *Geophysical Research*  
611 *Letters*, 35, 2008.  
612 Auclair, A. N.: Postfire regeneration of plant and soil organic pools in a *Picea mariana*–*Cladonia stellaris* ecosystem,  
613 *Canadian Journal of Forest Research*, 15, 279–291, 1985.  
614 Ballantyne, A. P., Axford, Y., Miller, G. H., Otto-Bliesner, B. L., Rosenbloom, N., and White, J. W.: The amplification  
615 of Arctic terrestrial surface temperatures by reduced sea-ice extent during the Pliocene, *Palaeogeography,*  
616 *Palaeoclimatology, Palaeoecology*, 386, 59–67, 2013.  
617 Ballantyne, A. P., Greenwood, D. R., Sinninghe Damsté, J. S., Csank, A. Z., Eberle, J. J., and Rybczynski, N.:  
618 Significantly warmer Arctic surface temperatures during the Pliocene indicated by multiple independent proxies,  
619 *Geology*, 38, 603–606, 2010.

Deleted:

Deleted: [

Deleted: ]

Deleted: .

624 Ballantyne, A. P., Ryczynski, N., Baker, P. A., Harington, C. R., and White, D.: Pliocene Arctic temperature  
625 constraints from the growth rings and isotopic composition of fossil larch, *Palaeogeography, Palaeoclimatology,*  
626 *Palaeoecology*, 242, 188–200, 2006.

627 Bendle, J. A., Weijers, J. W., Maslin, M. A., Sinninghe Damsté, J. S., Schouten, S., Hopmans, E. C., Boot, C. S., and  
628 Pancost, R. D.: Major changes in glacial and Holocene terrestrial temperatures and sources of organic carbon recorded  
629 in the Amazon fan by tetraether lipids, *Geochemistry, Geophysics, Geosystems*, 11, 2010.

630 Berg, E. E. and Chapin III, F. S.: Needle loss as a mechanism of winter drought avoidance in boreal conifers, *Canadian*  
631 *Journal of Forest Research*, 24, 1144–1148, 1994.

632 Bergeron, Y.: The influence of island and mainland lakeshore landscapes on boreal forest fire regimes, *Ecology*, 72,  
633 1980–1992, 1991.

634 Bergeron, Y., Cyr, D., Drever, C. R., Flannigan, M., Gauthier, S., Kneeshaw, D., Lauzon, È., Leduc, A., Goff, H. L.,  
635 Lesieur, D., and Logan, K.: Past, current, and future fire frequencies in Quebec's commercial forests: implications for  
636 the cumulative effects of harvesting and fire on age-class structure and natural disturbance-based management,  
637 *Canadian Journal of Forest Research*, 36, 2737–2744, 2006.

638 [Bonan, G. B.: Forests and Climate Change: Forcings, Feedbacks, and the Climate Benefits of Forests. \*Science\*, 320,](#)  
639 [1444–1449, 2008.](#)

640 Bouchard, M., Pothier, D., and Gauthier, S.: Fire return intervals and tree species succession in the North Shore region  
641 of eastern Quebec, *Canadian Journal of Forest Research*, 38, 1621–1633, 2008.

642 Brigham-Grette, J. and Carter, L. D.: Pliocene Marine Transgressions of Northern Alaska: Circumarctic Correlations  
643 and Paleoclimatic Interpretations, *Arctic*, 45, 74–89, 1992.

644 Brown, K. J. and Giesecke, T.: Holocene fire disturbance in the boreal forest of central Sweden, *Boreas*, 43, 639–651,  
645 2014.

646 Brown, K. J. and Power, M. J.: Charred particle analyses. In: *Encyclopedia of Quaternary Science*, Elias, S. (Ed.),  
647 Elsevier, Amsterdam, 2013.

648 Brown, M.: Fire and Ice: Fire Severity and Future Flammability in Alaskan Black Spruce Forests, *Fire Science Brief*,  
649 2008. 1–6, 2008.

650 Bush, E. and Lemmen, D.S.(eds): *Canada's Changing Climate Report*; Government of Canada, Ottawa, ON. 444 p.,  
651 2019

652 Busher, P. E.: Food Caching Behavior of Beavers (*Castor canadensis*): Selection and Use of Woody Species, *The*  
653 *American Midland Naturalist*, 135, 343–348, 1996.

654 [Clymo, R. S.: The Origin of Acidity in Sphagnum Bogs. \*The Bryologist\*, 67, 427–431, 1964.](#)

655 Côté, M., Ferron, J., and Gagnon, R.: Impact of seed and seedling predation by small rodents on early regeneration  
656 establishment of black spruce, *Canadian Journal of Forest Research*, 33, 2362–2371, 2003.

657 Csank, A. Z., Patterson, W. P., Eglington, B. M., Ryczynski, N., and Basinger, J. F.: Climate variability in the Early  
658 Pliocene Arctic: Annually resolved evidence from stable isotope values of sub-fossil wood, Ellesmere Island, Canada,  
659 *Palaeogeography, Palaeoclimatology, Palaeoecology*, 308, 339–349, 2011a.

Deleted: ¶

661 Csank, A. Z., Tripathi, A. K., Patterson, W. P., Eagle, R. A., Rybczynski, N., Ballantyne, A. P., and Eiler, J. M.:  
662 Estimates of Arctic land surface temperatures during the early Pliocene from two novel proxies, *Earth and Planetary*  
663 *Science Letters*, 304, 291–299, 2011b.

664 de Groot, W. J., Cantin, A. S., Flannigan, M. D., Soja, A. J., Gowman, L. M., and Newbery, A.: A comparison of  
665 Canadian and Russian boreal forest fire regimes, *Forest Ecology and Management*, 294, 23–34, 2013.

666 de Groot, W. J., Thomas, P. A., and Wein, R. W.: *Betula nana* L. and *Betula glandulosa* Michx, *Journal of Ecology*,  
667 85, 241–264, 1997.

668 De Jonge, C., Hopmans, E. C., Stadnitskaia, A., Rijpstra, W. I. C., Hofland, R., Tegelaar, E., and Sinninghe Damsté,  
669 J. S.: Identification of novel penta- and hexamethylated branched glycerol dialkyl glycerol tetraethers in peat using  
670 HPLC–MS 2, GC–MS and GC–SMB–MS, *Organic geochemistry*, 54, 78–82, 2013.

671 De Jonge, C., Hopmans, E. C., Zell, C. I., Kim, J.-H., Schouten, S., and Sinninghe Damsté, J. S.: Occurrence and  
672 abundance of 6-methyl branched glycerol dialkyl glycerol tetraethers in soils: Implications for palaeoclimate  
673 reconstruction, *Geochimica et Cosmochimica Acta*, 141, 97–112, 2014.

674 De Jonge, C., Stadnitskaia, A., Hopmans, E. C., Cherkashov, G., Fedotov, A., Streletskaia, I. D., Vasiliev, A. A., and  
675 Sinninghe Damsté, J. S.: Drastic changes in the distribution of branched tetraether lipids in suspended matter and  
676 sediments from the Yenisei River and Kara Sea (Siberia): Implications for the use of brGDGT-based proxies in coastal  
677 marine sediments, *Geochimica et Cosmochimica Acta*, 165, 200–225, 2015.

678 de Lafontaine, G. and Payette, S.: Shifting zonal patterns of the southern boreal forest in eastern Canada associated  
679 with changing fire regime during the Holocene, *Quaternary Science Reviews*, 30, 867–875, 2011.

680 Dowsett, H., Dolan, A., Rowley, D., Pound, M., Salzmann, U., Robinson, M., Chandler, M., Foley, K., and Haywood,  
681 A.: The PRISM4 (mid-Piacenzian) palaeoenvironmental reconstruction, *Climate of the Past*, doi:doi:10.5194/cp-12-  
682 1519-2016, 2016. 2016.

683 Estrada, S., Piepjohn, K., Frey, M. J., Reinhardt, L., Andruleit, H., and von Gosen, W.: Pliocene coal-seam fires on  
684 southern Ellesmere Island, Canadian Arctic, *Neues Jahrbuch für Geologie und Paläontologie - Abhandlungen*, 251,  
685 33–52, 2009.

686 Feng, R., Otto-Bliesner, B., Fletcher, T., Ballantyne, A., and Brady, E.: Contributions to Pliocene Arctic warmth from  
687 removal of anthropogenic aerosol and enhanced forest fire emissions, San Francisco, USA. 2016, PP33A-2344.

688 Feng, R., Otto-Bliesner, B. L., Fletcher, T. L., Tabor, C. R., Ballantyne, A. P., and Brady, E. C.: Amplified Late  
689 Pliocene terrestrial warmth in northern high latitudes from greater radiative forcing and closed Arctic Ocean gateways,  
690 *Earth and Planetary Science Letters*, 466, 129–138, 2017.

691 Flannigan, M., Stocks, B., Turetsky, M., and Wotton, M.: Impacts of climate change on fire activity and fire  
692 management in the circumboreal forest, *Global Change Biology*, 15, 549–560, 2009.

693 Fletcher, T., Feng, R., Telka, A. M., Matthews, J. V., and Ballantyne, A.: Floral dissimilarity and the influence of  
694 climate in the Pliocene High Arctic: Biotic and abiotic influences on five sites on the Canadian Arctic Archipelago,  
695 *Frontiers in Ecology and Evolution*, 5, 19, 2017.

**Deleted:** Dowsett, H. J., Cronin, T. M., Poore, R. Z., Thompson, R. S., Whatley, R. C., and Wood, A. M.: Micropaleontological evidence for increased meridional heat transport in the North Atlantic Ocean during the Pliocene, *Science*, 258, 1133–1136, 1992.¶  
Dowsett, H. J., Robinson, M. M., Haywood, A. M., Hill, D. J., Dolan, A. M., Stoll, D. K., Chan, W. L., Abe-Ouchi, A., Chandler, M. A., and Rosenbloom, N. A.: Assessing confidence in Pliocene sea surface temperatures to evaluate predictive models, *Nature Climate Change*, 2, 365–371, 2012.¶

705 Foster, L. C., Pearson, E. J., Juggins, S., Hodgson, D. A., Saunders, K. M., Verleyen, E., and Roberts, S. J.:  
706 Development of a regional glycerol dialkyl glycerol tetraether (GDGT)–temperature calibration for Antarctic and sub-  
707 Antarctic lakes, *Earth and Planetary Science Letters*, 433, 370–379, 2016.

708 Francis, J. and Skific, N.: Evidence linking rapid Arctic warming to mid-latitude weather patterns, *Philosophical*  
709 *Transactions of the Royal Society A: Mathematical, Physical and Engineering Sciences*, 373, 1–12, 2015.

710 [French, N. H., Whitley, M. A., and Jenkins, L. K.: Fire disturbance effects on land surface albedo in Alaskan tundra,](#)  
711 [Journal of Geophysical Research: Biogeosciences](#), 121, 841–854, 2016.

712 GBIF.org: GBIF Occurrence Download (Beaver Pond extant species) <http://doi.org/10.15468/dl.ertiqj> 1st February  
713 2017.

714 GBIF.org: GBIF Occurrence Download (*Betula*) <https://doi.org/10.15468/dl.akxgp5> 11th May 2018a.

715 GBIF.org: GBIF Occurrence Download (*Larix*) <https://doi.org/10.15468/dl.mfhnci> 11th May 2018b.

716 GBIF.org: GBIF Occurrence Download (*Picea*) <https://doi.org/10.15468/dl.wi7jdc> 11th May 2018c.

717 GBIF.org: GBIF Occurrence Download (*Pinus*) <https://doi.org/10.15468/dl.vwfjj2> 11th May 2018d.

718 Greene, G. A. and Daniels, L. D.: Spatial interpolation and mean fire interval analyses quantify historical mixed-  
719 severity fire regimes, *International Journal of Wildland Fire*, 26, 136–147, 2017.

720 Haarberg, O. and Rosell, F.: Selective foraging on woody plant species by the Eurasian beaver (*Castor fiber*) in  
721 Telemark, Norway, *Journal of Zoology*, 270, 201–208, 2006.

722 [Harrison, S., Bartlein, P. J., Brovkin, V., Houweling, S., Kloster, S., and Prentice, I. C.: The biomass burning](#)  
723 [contribution to climate-carbon-cycle feedback, Earth System Dynamics](#), 9, 663–677, 2018.

724 [Huang, S., Dahal, D., Liu, H., Jin, S., Young, C., Li, S., and Liu, S.: Spatiotemporal variation of surface shortwave](#)  
725 [forcing from fire-induced albedo change in interior Alaska, Canadian Journal of Forest Research](#), 45, 276–285, 2014.

726 Haywood, A. M., Dowsett, H. J., and Dolan, A. M.: Integrating geological archives and climate models for the mid-  
727 Pliocene warm period, *Nature communications*, 7, 1–14, 2016.

728 Higuera, P., Barnes, J. L., Chipman, M. L., Urban, M., and Hu, F. S.: The burning tundra: A look back at the last 6,000  
729 years of fire in the Noatak National Preserve, Northwestern Alaska, *Alaska Park Science*, 10, 37–41, 2011.

730 Higuera, P. E., Brubaker, L. B., Anderson, P. M., Hu, F. S., and Brown, T. A.: Vegetation mediated the impacts of  
731 postglacial climate change on fire regimes in the south-central Brooks Range, Alaska, *Ecological Monographs*, 79,  
732 201–219, 2009.

733 Hijmans, R. J., Cameron, S. E., Parra, J. L., Jones, P. G., and Jarvis, A.: Very high resolution interpolated climate  
734 surfaces for global land areas, *International Journal of Climatology*, 25, 1965–1978, 2005.

735 Hopmans, E. C., Schouten, S., and Sinninghe Damsté, J. S.: The effect of improved chromatography on GDGT-based  
736 palaeoproxies, *Organic Geochemistry*, 93, 1–6, 2016.

737 Hu, F. S., Higuera, P. E., Walsh, J. E., Chapman, W. L., Duffy, P. A., Brubaker, L. B., and Chipman, M. L.: Tundra  
738 burning in Alaska: Linkages to climatic change and sea ice retreat, *Journal of Geophysical Research: Biogeosciences*,  
739 115, 2010.

740 Huguet, C., Hopmans, E. C., Febo-Ayala, W., Thompson, D. H., Sinninghe Damsté, J. S., and Schouten, S.: An  
741 improved method to determine the absolute abundance of glycerol dibiphytanyl glycerol tetraether lipids, *Organic*  
742 *Geochemistry*, 37, 1036–1041, 2006.

743 Hwang, Y. T., Frierson, D. M., and Kay, J. E.: Coupling between Arctic feedbacks and changes in poleward energy  
744 transport, *Geophysical Research Letters*, 38, 2011.

745 Jacquelyn, K. S., Adrianna, C. F., Herman, H. S., Amanda, H.-H., Alexander, K., Tatiana, L., Dmitry, E., and Elena,  
746 S.: Fire disturbance and climate change: implications for Russian forests, *Environmental Research Letters*, 12, 035003,  
747 2017.

748 Jenkins, S. H.: Seasonal and year-to-year differences in food selection by beavers, *Oecologia*, 44, 112–116, 1979.

749 [Jin, Y., Randerson, J. T., Goulden, M. L., and Goetz, S. J.: Post-fire changes in net shortwave radiation along a](#)  
750 [latitudinal gradient in boreal North America, \*Geophysical Research Letters\*, 39, L13403, 2012.](#)

751 Johnstone, J. F., Chapin, F. S., Hollingsworth, T. N., Mack, M. C., Romanovsky, V., and Turetsky, M.: Fire, climate  
752 change, and forest resilience in interior Alaska, *Canadian Journal of Forest Research*, 40, 1302–1312, 2010a.

753 Johnstone, J. F., Hollingsworth, T. N., Chapin, F. S., and Mack, M. C.: Changes in fire regime break the legacy lock  
754 on successional trajectories in Alaskan boreal forest, *Global Change Biology*, 16, 1281–1295, 2010b.

755 Johnstone, J. F. and Kasischke, E. S.: Stand-level effects of soil burn severity on postfire regeneration in a recently  
756 burned black spruce forest, *Canadian Journal of Forest Research*, 35, 2151–2163, 2005.

757 Jones, P. D. and Moberg, A.: Hemispheric and large-scale surface air temperature variations: An extensive revision  
758 and an update to 2001, *Journal of Climate*, 16, 206–223, 2003.

759 Kasischke, E. S. and Turetsky, M. R.: Recent changes in the fire regime across the North American boreal region—  
760 spatial and temporal patterns of burning across Canada and Alaska, *Geophysical research letters*, 33, 2006.

761 Kasischke, E. S., Turetsky, M. R., Ottmar, R. D., French, N. H., Hoy, E. E., and Kane, E. S.: Evaluation of the  
762 composite burn index for assessing fire severity in Alaskan black spruce forests, *International Journal of Wildland*  
763 *Fire*, 17, 515–526, 2008.

764 Kasischke, E. S., Williams, D., and Barry, D.: Analysis of the patterns of large fires in the boreal forest region of  
765 Alaska, *International Journal of Wildland Fire*, 11, 131–144, 2002.

766 Kharuk, V. I., Dvinskaya, M. L., Petrov, I. A., Im, S. T., and Ranson, K. J.: Larch forests of Middle Siberia: long-term  
767 trends in fire return intervals, *Regional Environmental Change*, doi: 10.1007/s10113-016-0964-9, 2016. 1–9, 2016.

768 Kharuk, V. I., Ranson, K. J., Dvinskaya, M. L., and Im, S. T.: Wildfires in northern Siberian larch dominated  
769 communities, *Environmental Research Letters*, 6, 045208, 2011.

770 Kobayashi, M., Nemilostiv, Y. P., Zyryanova, O. A., Kajimoto, T., Matsuura, Y., Yoshida, T., Satoh, F., Sasa, K., and  
771 Koike, T.: Regeneration after forest fires in mixed conifer broad-leaved forests of the Amur region in far eastern  
772 Russia: the relationship between species specific traits against fire and recent fire regimes, *Eurasian Journal of Forest*  
773 *Research*, 10, 51–58, 2007.

774 Kooijman, A. and Westhoff, V.: Variation in habitat factors and species composition of *Scorpidium scorpioides*  
775 communities in NW-Europe, *Plant Ecology*, 117, 133–150, 1995.

776 Kooijman, A. M. and Paulissen, M. P. C. P.: Higher acidification rates in fens with phosphorus enrichment, *Applied*  
777 *Vegetation Science*, 9, 205–212, 2006.

778 Lifton, N., Sato, T., and Dunai, T. J.: Scaling in situ cosmogenic nuclide production rates using analytical  
779 approximations to atmospheric cosmic-ray fluxes, *Earth and Planetary Science Letters*, 386, 149–160, 2014.

780 Lisiecki, L. E. and Raymo, M. E.: A Plio-Pleistocene stack of 57 globally distributed benthic  $\delta^{18}\text{O}$  records,  
781 *Paleoceanography*, 20, 2005.

782 [Liu, Z., Ballantyne, A. P., and Cooper, L. A.: Biophysical feedback of global forest fires on surface temperature,](#)  
783 [Nature Communications](#), 10, 214, 2019.

784 Loomis, S. E., Russell, J. M., Ladd, B., Street-Perrott, F. A., and Sinninghe  
785 Damsté, J. S.: Calibration and application of the branched GDGT temperature proxy on East African lake sediments,  
786 *Earth and Planetary Science Letters*, 357, 277–288, 2012.

787 Lorimer, C. G.: The Presettlement Forest and Natural Disturbance Cycle of Northeastern Maine, *Ecology*, 58, 139–  
788 148, 1977.

789 Luthi, D., Le Floch, M., Bereiter, B., Blunier, T., Barnola, J.-M., Siegenthaler, U., Raynaud, D., Jouzel, J., Fischer,  
790 H., Kawamura, K., and Stocker, T. F.: High-resolution carbon dioxide concentration record 650,000–800,000 years  
791 before present, *Nature*, 453, 379–382, 2008.

792 Lynch, J. A., Clark, J. S., Bigelow, N. H., Edwards, M. E., and Finney, B. P.: Geographic and temporal variations in  
793 fire history in boreal ecosystems of Alaska, *Journal of Geophysical Research: Atmospheres*, 107, FFR 8-1–FFR 8-17,  
794 2002.

795 Mack, M. C., Bret-Harte, M. S., Hollingsworth, T. N., Jandt, R. R., Schuur, E. A. G., Shaver, G. R., and Verbyla, D.  
796 L.: Carbon loss from an unprecedented Arctic tundra wildfire, *Nature*, 475, 489–492, 2011.

797 Marshall, J., Armour, K. C., Scott, J. R., Kostov, Y., Hausmann, U., Ferreira, D., Shepherd, T. G., and Bitz, C. M.:  
798 The ocean's role in polar climate change: asymmetric Arctic and Antarctic responses to greenhouse gas and ozone  
799 forcing, *Philosophical Transactions of the Royal Society of London A: Mathematical, Physical and Engineering*  
800 *Sciences*, 372, 20130040, 2014.

801 Matthews Jr, J. V. and Oviden, L. E.: Late Tertiary plant macrofossils from localities in Arctic/sub- Arctic North  
802 America: a review of the data, *Arctic*, 43, 364–392, 1990.

803 Matthews, J. V. J. and Fyles, J. G.: Late Tertiary plant and arthropod fossils from the High Terrace Sediments on the  
804 Fosheim Peninsula of Ellesmere Island (Northwest Territories, District of Franklin), *Geological Survey of Canada*,  
805 *Bulletin*, 529, 295–317, 2000.

806 Mattson, M. D.: Acid lakes and rivers. In: *Environmental Geology*, Springer Netherlands, Dordrecht, 1999.

807 McAndrews, J. H., Berti, A. A., and Norris, G.: Key to the Quaternary pollen and spores of the Great Lakes region,  
808 1973. 1973.

809 Miller, G. H., Alley, R. B., Brigham-Grette, J., Fitzpatrick, J. J., Polyak, L., Serreze, M. C., and White, J. W. C.: Arctic  
810 amplification: can the past constrain the future?, *Quaternary Science Reviews*, 29, 1779–1790, 2010.

811 Mitchell, W. T., Rybczynski, N., Schröder-Adams, C., Hamilton, P. B., Smith, R., and Douglas, M.: Stratigraphic and  
812 Paleoenvironmental Reconstruction of a Mid-Pliocene Fossil Site in the High Arctic (Ellesmere Island, Nunavut):  
Evidence of an Ancient Peatland with Beaver Activity, *Arctic*, 69, 185–204, 2016.



813 Moore, P. D., Webb, J. A., and Collison, M. E.: Pollen analysis, Blackwell Scientific Publications, Oxford, 1991.

814 Naafs, B., Inglis, G., Zheng, Y., Amesbury, M., Biester, H., Bindler, R., Blewett, J., Burrows, M., del Castillo Torres,  
815 D., and Chambers, F. M.: Introducing global peat-specific temperature and pH calibrations based on brGDGT bacterial  
816 lipids, *Geochimica et Cosmochimica Acta*, 208, 285–301, 2017.

817 Niemann, H., Stadnitskaia, A., Wirth, S., Gilli, A., Anselmetti, F., Sinninghe Damsté, J., Schouten, S., Hopmans, E.,  
818 and Lehmann, M.: Bacterial GDGTs in Holocene sediments and catchment soils of a high Alpine lake: application of  
819 the MBT/CBT-paleothermometer, *Climate of the Past*, 8, 889-906, 2012.

820 Niklasson, M. and Drakenberg, B.: A 600-year tree-ring fire history from Norra Kvills National Park, southern  
821 Sweden: implications for conservation strategies in the hemiboreal zone, *Biological Conservation*, 101, 63–71, 2001.

822 Niklasson, M. and Granström, A.: Fire in Sweden – History, Research, Prescribed Burning and Forest Certification,  
823 *International Forest Fire News*, 30, 80–83, 2004.

824 Niklasson, M. and Granström, A.: Numbers and sizes of fires: Long-term spatially explicit fire history in a Swedish  
825 boreal landscape, *Ecology*, 81, 1484–1499, 2000.

826 Otto-Bliessner, B. L. and Upchurch Jr, G. R.: Vegetation-induced warming of high-latitude regions during the Late  
827 Cretaceous period, *Nature*, 385, 804, 1997.

828 Pagani, M., Liu, Z., LaRiviere, J., and Ravelo, A. C.: High Earth-system climate sensitivity determined from Pliocene  
829 carbon dioxide concentrations, *Nature Geoscience*, 3, 27–30, 2010.

830 Pearson, E. J., Juggins, S., Talbot, H. M., Weckström, J., Rosén, P., Ryves, D. B., Roberts, S. J., and Schmidt, R.: A  
831 lacustrine GDGT-temperature calibration from the Scandinavian Arctic to Antarctic: Renewed potential for the  
832 application of GDGT-paleothermometry in lakes, *Geochimica et Cosmochimica Acta*, 75, 6225–6238, 2011.

833 Peterse, F., Prins, M. A., Beets, C. J., Troelstra, S. R., Zheng, H., Gu, Z., Schouten, S., and Sinninghe Damsté, J. S.:  
834 Decoupled warming and monsoon precipitation in East Asia over the last deglaciation, *Earth and Planetary Science  
835 Letters*, 301, 256–264, 2011.

836 Powers, L. A., Werne, J. P., Johnson, T. C., Hopmans, E. C., Sinninghe Damsté, J. S., and Schouten, S.: Crenarchaeotal  
837 membrane lipids in lake sediments: A new paleotemperature proxy for continental paleoclimate reconstruction?,  
838 *Geology*, 32, 613–616, 2004.

839 R Core Team: R: A language and environment for statistical computing. R Foundation for Statistical Computing,  
840 Vienna, Austria, 2016.

841 Racine, C. H., Johnson, L. A., and Viereck, L. A.: Patterns of Vegetation Recovery after Tundra Fires in Northwestern  
842 Alaska, U.S.A, *Arctic and Alpine Research*, 19, 461–469, 1987.

843 [Randerson, J., Liu, H., Flanner, M., Chambers, S., Jin, Y., Hess, P., Pfister, G., Mack, M., Treseder, K., and Welp, L.:  
844 The impact of boreal forest fire on climate warming. \*Science\*, 314, 1130–1132, 2006.](#)

845 Robinson, M. M.: New Quantitative Evidence of Extreme Warmth in the Pliocene Arctic, *Stratigraphy*, 6, 265–275,  
846 2009.

847 Rogers, B. M., Soja, A. J., Goulden, M. L., and Randerson, J. T.: Influence of tree species on continental differences  
848 in boreal fires and climate feedbacks, *Nature Geoscience*, 8, 228–234, 2015.

849 Royer, D. L., Berner, R. A., and Park, J.: Climate sensitivity constrained by CO<sub>2</sub> concentrations over the past 420  
850 million years, *Nature*, 446, 530-532, 2007.

851 Russell, J. M., Hopmans, E. C., Loomis, S. E., Liang, J., and Sinninghe Damsté, J. S.: Distributions of 5- and 6-methyl  
852 branched glycerol dialkyl glycerol tetraethers (brGDGTs) in East African lake sediment: Effects of temperature, pH,  
853 and new lacustrine paleotemperature calibrations, *Geochimica et Cosmochimica Acta*, 117, 56–69, 2018.

854 Ryan, K. C.: Dynamic interactions between forest structure and fire behavior in boreal ecosystems, *Silva Fennica*, 36,  
855 13–39, 2002.

856 Rybczynski, N., Gosse, J. C., Richard Harington, C., Wogelius, R. A., Hidy, A. J., and Buckley, M.: Mid-Pliocene  
857 warm-period deposits in the High Arctic yield insight into camel evolution, *Nature Communications*, 4, 1–9, 2013.

858 ~~Salzmann, U., Haywood, A. M., Lunt, D., Valdes, P., and Hill, D.: A new global biome reconstruction and data-model  
859 comparison for the middle Pliocene, *Global Ecology and Biogeography*, 17, 432–447, 2008.~~

860 [Schultz, N. M., Lawrence, P. J., and Lee, X.: Global satellite data highlights the diurnal asymmetry of the surface  
861 temperature response to deforestation, \*Journal of Geophysical Research: Biogeosciences\*, 122, 903–917, 2017.](#)

862 Sinninghe Damsté, J. S.: Spatial heterogeneity of sources of branched tetraethers in shelf systems: The geochemistry  
863 of tetraethers in the Berau River delta (Kalimantan, Indonesia), *Geochimica et Cosmochimica Acta*, 186, 13–31, 2016.

864 Sinninghe Damsté J.S., Rijpstra W.I.C., Foessel B.U., Huber K., Overmann J., Nakagawa S., Joong Jae Kim, Dunfield  
865 P.F. Dedysh S.N., Villanueva L. (2018) An overview of the occurrence of ether- and ester-linked iso-diabolic acid  
866 membrane lipids in microbial cultures of the Acidobacteria: Implications for brGDGT palaeoproxies for temperature  
867 and pH. *Organic Geochemistry*, 124, 63–76.

868 Sinninghe Damsté, J. S., Rijpstra, W. I. C., Hopmans, E. C., Foessel, B. U., Wüst, P. K., Overmann, J., Tank, M.,  
869 Bryant, D. A., Dunfield, P. F., Houghton, K., and Stott, M. B.: Ether- and Ester-Bound iso-Diabolic Acid and Other  
870 Lipids in Members of Acidobacteria Subdivision 4, *Applied and Environmental Microbiology*, 80, 5207–5218, 2014.

871 Sinninghe Damsté, J. S., Rijpstra, W. I. C., Hopmans, E. C., Weijers, J. W., Foessel, B. U., Overmann, J., and Dedysh,  
872 S. N.: 13, 16-Dimethyl octacosanedioic acid (iso-diabolic acid), a common membrane-spanning lipid of Acidobacteria  
873 subdivisions 1 and 3, *Applied and Environmental Microbiology*, 77, 4147–4154, 2011.

874 Stap, L. B., de Boer, B., Ziegler, M., Bintanja, R., Lourens, L. J., and van de Wal, R. S.: CO<sub>2</sub> over the past 5 million  
875 years: Continuous simulation and new  $\delta^{11}\text{B}$ -based proxy data, *Earth and Planetary Science Letters*, 439, 1–10, 2016.

876 [Stone, R., Anderson, G., Shettle, E., Andrews, E., Loukachine, K., Dutton, E., Schaaf, C., and Roman, M.: Radiative  
877 impact of boreal smoke in the Arctic: Observed and modeled, \*Journal of Geophysical Research: Atmospheres\*, 113,  
878 2008.](#)

879 Swann, A. L., Fung, I. Y., Levis, S., Bonan, G. B., and Doney, S. C.: Changes in Arctic vegetation amplify high-  
880 latitude warming through the greenhouse effect, *Proceedings of the National Academy of Sciences of the United States*  
881 *of America*, 107, 1295-1300, 2010.

882 Tedford, R. H. and Harington, C. R.: An Arctic mammal fauna from the early Pliocene of North America, *Nature*,  
883 425, 388–390, 2003.

884 Van Wagner, C. E., Finney, M. A., and Heathcott, M.: Historical fire cycles in the Canadian Rocky Mountain parks,  
885 *Forest Science*, 52, 704-717, 2006.

**Deleted:** Salzmann, U., Dolan, A. M., Haywood, A. M., Chan, W.-L., Voss, J., Hill, D. J., Abe-Ouchi, A., Otto-Bliesner, B., Bragg, F. J., and Chandler, M. A.: Challenges in quantifying Pliocene terrestrial warming revealed by data-model discord, *Nature Climate Change*, 3, 969, 2013.¶

**Deleted:** Shellito, C. J., Lamarque, J.-F. o., and Sloan, L. C.: Early Eocene Arctic climate sensitivity to  $p\text{CO}_2$  and basin geography, *Geophysical Research Letters*, 36, 2009.¶

894 Wang, X., Rycbizynski, N., Harington, C. R., White, S. C., and Tedford, R. H.: A basal ursine bear (*Protarctos*  
895 *abstrusus*) from the Pliocene High Arctic reveals Eurasian affinities and a diet rich in fermentable sugars, *Scientific*  
896 *reports*, 7, 17722, 2017.

897 [Ward, D., Kloster, S., Mahowald, N., Rogers, B., Randerson, J., and Hess, P.: The changing radiative forcing of fires:](#)  
898 [global model estimates for past, present and future, \*Atmospheric Chemistry and Physics\*, 12, 10857–10886, 2012.](#)

899 Warden, L., Jung-Hyun, K., Zell, C., Vis, G.-J., de Stigter, H., Bonnin, J., and Sinninghe Damsté, J. S.: Examining  
900 the provenance of branched GDGTs in the Tagus River drainage basin and its outflow into the Atlantic Ocean over  
901 the Holocene to determine their usefulness for paleoclimate applications, *Biogeosciences*, 13, 5719, 2016.

902 Weijers, J. W., Schefuß, E., Schouten, S., and Sinninghe Damsté, J. S.: Coupled thermal and hydrological evolution  
903 of tropical Africa over the last deglaciation, *Science*, 315, 1701–1704, 2007a.

904 Weijers, J. W., Schouten, S., van den Donker, J. C., Hopmans, E. C., and Sinninghe Damsté, J. S.: Environmental  
905 controls on bacterial tetraether membrane lipid distribution in soils, *Geochimica et Cosmochimica Acta*, 71, 703-713,  
906 2007b.

907 Weijers, J. W. H., Schouten, S., van den Donker, J. C., Hopmans, E. C., and Sinninghe Damsté, J. S.: Environmental  
908 controls on bacterial tetraether membrane lipid distribution in soils, *Geochimica et Cosmochimica Acta*, 71, 703-713,  
909 2007c.

910 Whitman, E., Battlori, E., Parisien, M. A., Miller, C., Coop, J. D., Krawchuk, M. A., Chong, G. W., and Haire, S. L.:  
911 The climate space of fire regimes in north-western North America, *Journal of Biogeography*, 42, 1736–1749, 2015.

912 Wright, C. S. and Agee, J. K.: Fire and vegetation history in the eastern Cascade Mountains, Washington, *Ecological*  
913 *Applications*, 14, 443–459, 2004.

914 Yang, G., Zhang, C. L., Xie, S., Chen, Z., Gao, M., Ge, Z., and Yang, Z.: Microbial glycerol dialkyl glycerol tetraethers  
915 from river water and soil near the Three Gorges Dam on the Yangtze River, *Organic Geochemistry*, 56, 40–50, 2013.

916 Yarie, J.: Forest fire cycles and life tables: a case study from interior Alaska, *Canadian Journal of Forest Research*,  
917 11, 554–562, 1981.

918 Young, A. M., Higuera, P. E., Duffy, P. A., and Hu, F. S.: Climatic thresholds shape northern high-latitude fire regimes  
919 and imply vulnerability to future climate change, *Ecography*, 40, 606–617, 2017.

920 Zech, R., Gao, L., Tarozo, R., and Huang, Y.: Branched glycerol dialkyl glycerol tetraethers in Pleistocene loess-  
921 paleosol sequences: three case studies, *Organic geochemistry*, 53, 38–44, 2012.

922 Zell, C., Kim, J.-H., Moreira-Turcq, P., Abril, G., Hopmans, E. C., Bonnet, M.-P., Sobrinho, R. L., and Sinninghe  
923 Damsté, J. S.: Disentangling the origins of branched tetraether lipids and crenarchaeol in the lower Amazon River:  
924 Implications for GDGT-based proxies, *Limnology and Oceanography*, 58, 343–353, 2013.

925 [Zhang, Y., Forrister, H., Liu, J., Dibb, J., Anderson, B., Schwarz, J. P., Perring, A. E., Jimenez, J. L., Campuzano-](#)  
926 [Jost, P., Wang, Y., Nenes, A., and Weber, R. J.: Top-of-atmosphere radiative forcing affected by brown carbon in the](#)  
927 [upper troposphere, \*Nature Geosci.\* 10, 486-489, 2017.](#)

928 [Zheng, J., Zhang, Q., Li, Q., Zhang, Q., and Cai, M.: Contribution of sea ice albedo and insulation effects to Arctic](#)  
929 [amplification in the EC-Earth Pliocene simulation, \*Climate of the Past\*, 15, 291–305, 2019.](#)

930 Zhu, C., Weijers, J. W., Wagner, T., Pan, J.-M., Chen, J.-F., and Pancost, R. D.: Sources and distributions of tetraether  
931 lipids in surface sediments across a large river-dominated continental margin, *Organic Geochemistry*, 42, 376–386,  
932 2011.

933 Zink, K.-G., Vandergoes, M. J., Mangelsdorf, K., Dieffenbacher-Krall, A. C., and Schwark, L.: Application of  
934 bacterial glycerol dialkyl glycerol tetraethers (GDGTs) to develop modern and past temperature estimates from New  
935 Zealand lakes, *Organic Geochemistry*, 41, 1060–1066, 2010.

936

**Table 1. Modern and recent Holocene fire return interval reconstructions for the candidate analogous regions considered in this study.**

Region	Modern		Reference	Recent Holocene		Reference
Alaskan Tundra	Seward Peninsula	273*	Kasischke et al. (2002)	Up-Valley	263	Higuera et al. (2011)
	Nulato Hills	306*		Down-valley	142	
Alaskan Boreal	Porcupine/ Upper Yukon (Central)	~100	Yarie (1981)			
	Sites near Fairbanks, and Delta Junction (Central)	70130	Johnstone et al. (2010a); Johnstone et al. (2010b); Johnstone and Kasischke (2005)			
	Kenai Peninsula		Lynch et al. (2002)	Interior Alaska and Kenai Peninsula	198 ± 90	Lynch et al. (2002)
	Yukon river Lowlands	120	Kasischke et al. (2002)	Brooks Range	145	Higuera et al. (2009)
	Kuskokwim Mountains	218				
	Yukon-Tanama Uplands	330				
	Tanana- Kuskokwim Lowlands	178				
	Kobuk Ridges and Valleys	175				
	Davidson Mountains	403				
	North Ogilive Mountains	112				
	Ray Mountains	109				
	Yukon-Old Crow Basin	81				

Western North America	Darkwoods, British Columbia	~69	Greene and Daniels (2017)			
	Cascade Mountains, Washington	~27	Wright and Agee (2004)			
	Desolation Peak, Washington Coastal type	108-137				
	Desolation Peak, Washington Interior type	~52				
Eastern North America	Quebec – west	~270*	Bouchard et al. (2008)	Maine	≥ 800	Lorimer (1977)
	Quebec – east	>500*				
				Quebec – “Spruce zone”	570	de Lafontaine and Payette (2011)
				Quebec – “Fir zone”	>1000	
	Quebec – Abitibi northwest	418*	Bergeron et al. (2006 post-1940)^	Quebec – Abitibi northwest	189	Bergeron et al. (2006 post-1940)^
	Quebec – Abitibi southwest	388*		Quebec – Abitibi southwest	165	
	Quebec – Abitibi east	418*		Quebec – Abitibi east	141	
	Quebec – Abitibi southeast	2083*		Quebec – Abitibi southeast	257	
Quebec – Temiscamingue north	2083*	Quebec – Temiscamingue north		220		

	Quebec – Temiscamingue south	2777*		Quebec – Temiscamingue south	313	
	Quebec – Waswanipi	418*		Quebec – Waswanipi	128	
	Quebec – Central Quebec	388*		Quebec – Central Quebec	150	
	Quebec – North Shore	645*		Quebec – North Shore	281	
	Quebec – Gaspésia	488*		Quebec – Gaspésia	161	
	Quebec – northwestern lakeshore	99 <sup>†</sup>	Bergeron (1991)	Quebec – northwestern lakeshore	63 <sup>†</sup>	Bergeron (1991)
	Quebec – northwestern lake island	112 <sup>†</sup>		Quebec – northwestern – lake island	74 <sup>†</sup>	
Fennoscandia	Sweden	*	Niklasson and Drakenberg (2001); Niklasson and Granström (2004)	North Sweden	50-150	Niklasson and Granström (2004); Niklasson and Granström (2000)
				Southern Sweden	20	
	Central Sweden	*	Brown and Giesecke (2014)	Central Sweden - Klotjärnen	180	Brown and Giesecke (2014)
			Central Sweden - Holtjärnen	240		
Siberian Plateau	Northern	300	Kharuk et al. (2016); Kharuk et al. (2011)			
	Southern	80				
	Mean (64-71°N)	110				

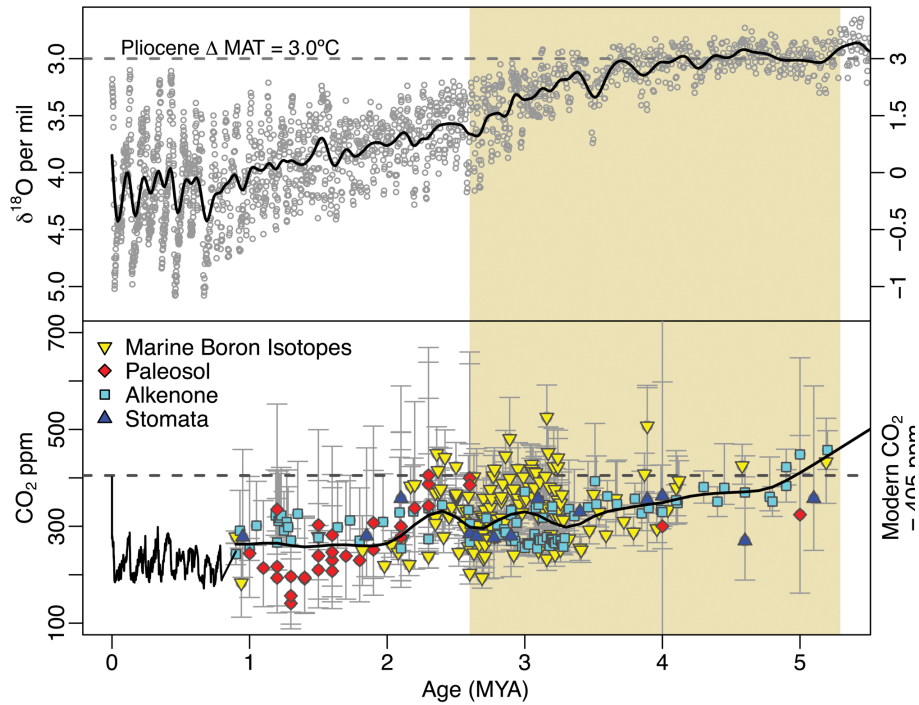
939 ^ = The reciprocal converted from burn rate (%) (see Van Wagner et al., 2006)

940 \* = Estimates likely effected in some areas by human activity. In such instances Recent Holocene is preferred.

941 † = Fire cycle

942 ‡ = 'Recent' here refers to records that (or have distinct sections that) begin after the end of the Holocene Climate

943 Optima and end near present



945

946

947

948

949

950

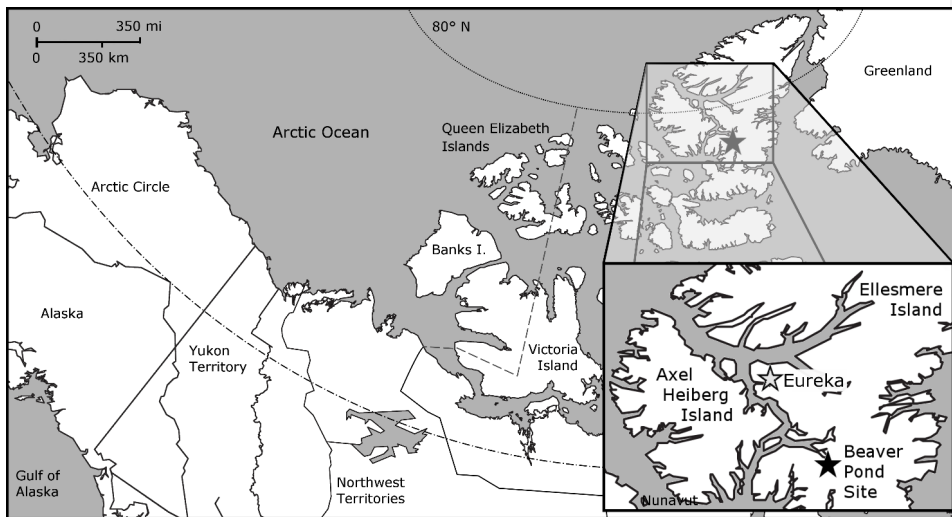
951

952

Figure 1: Global temperatures and atmospheric CO<sub>2</sub> concentration spanning the last 5 million years of Earth's history. Mean annual temperatures (MAT) are inferred from compiled δ<sup>18</sup>O foraminifera data (Lisiecki and Raymo, 2005) and plotted as anomalies from present (top panel). Modern atmospheric CO<sub>2</sub> measurements (NOAA/ESRL), and ice core observations from EPICA (Luthi et al., 2008) are compared with proxy estimates (bottom panel; see Table S1) for the Pliocene Epoch indicated with beige shading. Smoothed curves have been fit to highlight trends in pCO<sub>2</sub> and temperature during the Pliocene.



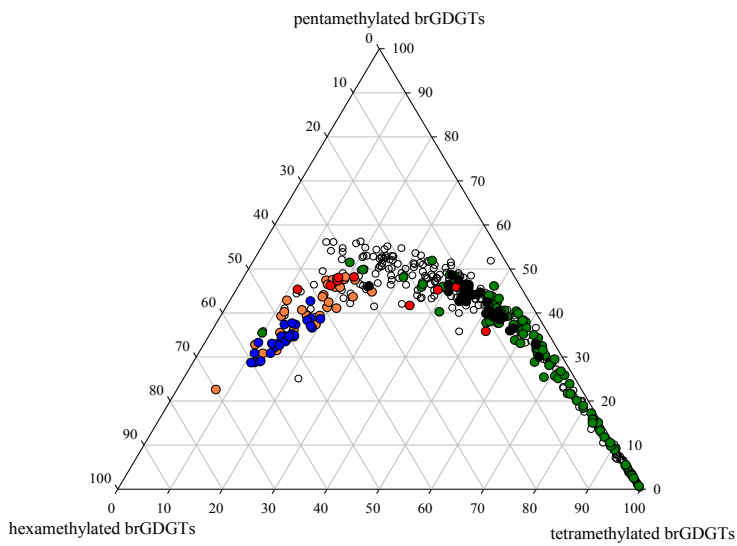
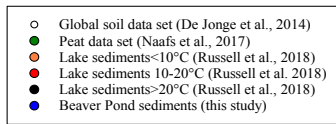
953



954

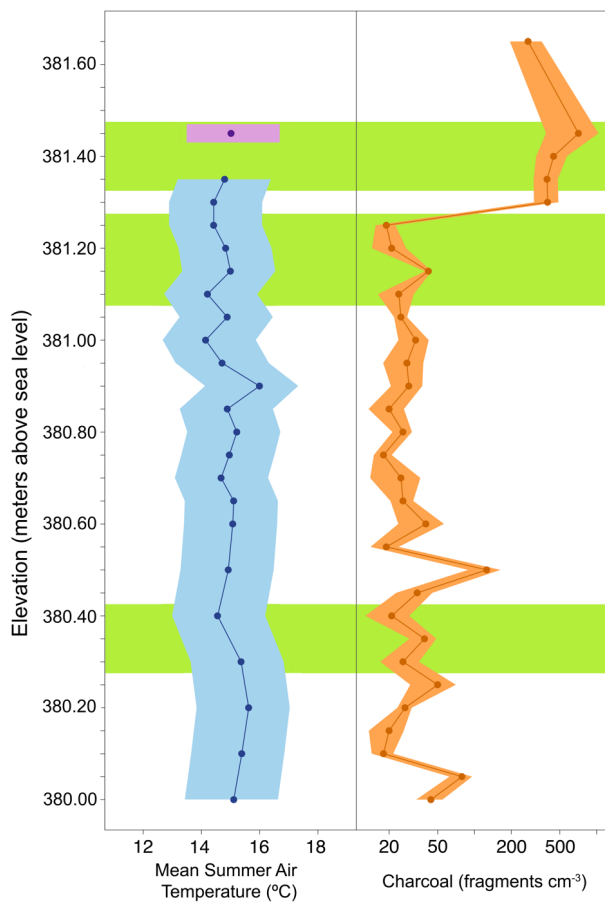
955 **Figure 2. Map of the Canadian Arctic Archipelago, highlighting the location of the Beaver Pond Site (Black**  
956 **Star; 78° 33' N; 82° 25' W) and Eureka Climate Station (Grey Star; 80° 13' N, 86° 11' W – used for modern**  
957 **climate comparison) on west-central Ellesmere Island.**

958



959  
 960 **Figure 3.** A ternary plot illustrating the fractional abundances of the tetra- (Ia-c), penta (IIa-c and II'a-c), and  
 961 hexamethylated (IIIa-c and III'a-c) brGDGTs. The global soil dataset (open circles; De Jonge et al., 2014), the  
 962 global peat samples (green circles; Naafs et al., 2017), and lake sediments from East Africa (black circles  
 963 indicate samples from lakes >20°C, red circles indicate samples from lakes between 10–20°C and orange circles  
 964 designate samples from lakes <10°C; Russell et al., 2018) are included for comparison with the Beaver Pond  
 965 sediments (blue circles; this study).

966

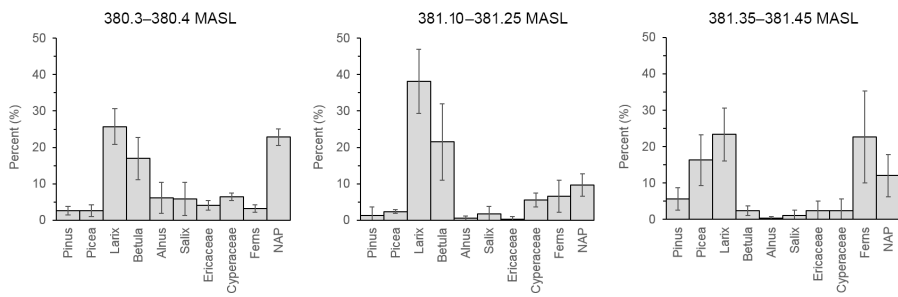


967

968 **Figure 4. Reconstruction of mean summer temperature and fire for the Canadian High Arctic during the**  
 969 **Pliocene. Mean summer air temperature reconstructed from a brGDGT based proxy (blue;  $\pm 2 \sigma$ ) and relative**  
 970 **2010 data point in approximate relative position (purple;  $\pm 2 \sigma$ ). Charcoal counts reported as the number of**  
 971 **fragments per volume (fragments  $\text{cm}^{-3}$ ) of peat (Orange  $\pm 2 \sigma$ ). Green boxes indicate relative depths of pollen**  
 972 **sampling. Elevation of the deposit is reported as meters above sea level. (Data: Table S3)**

973  
974  
975

(A)



976

977

(B)

978

979

980

981

982

983

984

985

986

987

988

989

990

991

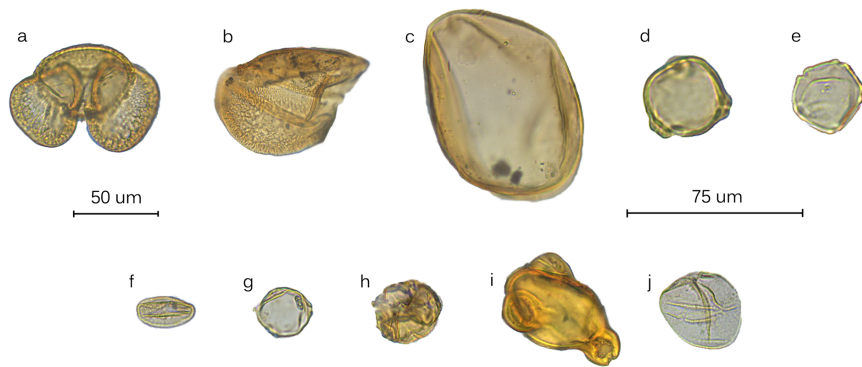
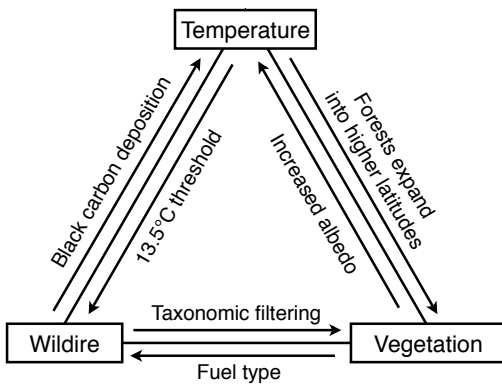
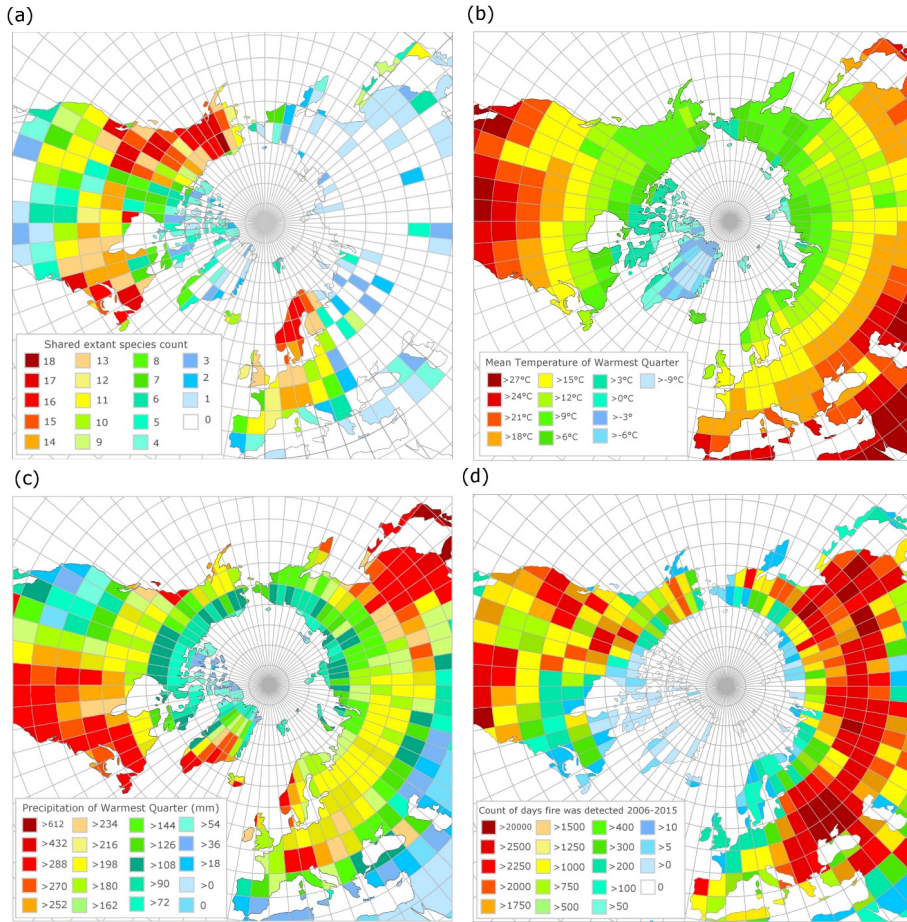


**Figure 5. (A) Bar charts showing the relative pollen abundance in each portion of the section (error bars = 95% confidence intervals; MASL- Meters Above Sea Level). (B). Pollen plate of select grains encountered in the BP section: (a) *Pinus*, (b) half a *Picea* grain, (c) *Larix*, (d) *Betula*, (e) *Alnus*, (f) *Salix*, (g) *Myrica*, (h) ericaceous grain, (i) *Epilobium*, and (j) *Cyperaceae*. 50um scale = (a-c), 75um scale = (d-j).**



992  
993

Figure 6: Examples of the feedbacks between temperature, vegetation and wildfire at the Beaver Pond site



995 **Figure 7. (a) Modern geographic distribution of observed occurrences of species common to the Beaver Pond**  
 996 **species list, (b) Mean temperature of the warmest quarter (summer average) derived from WorldClim, (c)**  
 997 **Mean precipitation of the warmest quarter (summer rain) derived from WorldClim, (d) Count of unique fire**  
 998 **pixels detected per day, over 10 years from MODIS 6 Fire Product, normalized by area of the latitude by**  
 999 **longitude grid.**